

INSTITUTE OF SCIENCES AND ENGINEERING

AUTOMOTIVE MECHATRONICS AND INTELLIGENT VEHICLES

MASTER OF SCIENCE PROGRAM



THEORETICAL AND EXPERIMENTAL ANALYSES OF ACTIVE SUSPENSION  
USING LQR, GROUNDHOOK AND SKYHOOK CONTROL METHODS

A Thesis

submitted by

HALİL KILIÇ

in partial fulfilment of the requirements for the degree of

MASTER OF SCIENCE

June 2019

THEORETICAL AND EXPERIMENTAL ANALYSES OF ACTIVE SUSPENSION  
USING LQR, GROUNDHOOK AND SKYHOOK CONTROL METHODS

A Thesis

by HALİL KILIÇ

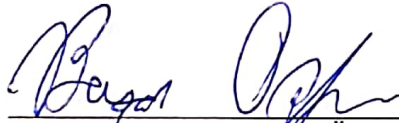
submitted to the Institute of Sciences and Engineering of

OKAN UNIVERSITY

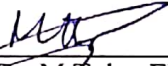
In partial fulfilment of the requirements for the degree of

MASTER OF SCIENCE

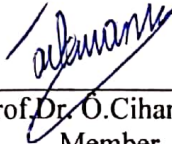
Approved by:



Asst.Prof.Dr. Başar ÖZKAN  
Supervisor



Asst.Prof.Dr. M. Tolga EMİRLER  
Member



Asst.Prof.Dr. Ö.Cihan KIVANÇ  
Member

June 2019

## ABSTRACT

### THEORETICAL AND EXPERIMENTAL ANALYSES OF ACTIVE SUSPENSION USING LQR, GROUNDHOOK AND SKYHOOK CONTROL METHODS

Suspension systems are used to isolate vehicles from road disturbances and allow damping of the incentives in vehicles. In this system, the wheel, axle and vehicle body are connected together. It is necessary to maintain a constant contact between the tires of a vehicle and the road. At this point, passive suspensions and handling are insufficient for driving comfort. The fast growing developments specially in the fields of computer, electronics and control systems have been very important in optimizing and developing the systems that contain performance, safety and comfort elements in vehicles. One of these important systems is vehicle suspension systems. The aim of this proposed research is to design and implement linear quadratic regulator (LQR), Skyhook and Groundhook algorithm for active suspension control. For the purpose of this study the performance of LQR, skyhook and groundhook controlled active suspension were compared by using Quanser active suspension test device's quarter vehicle model. In this study, MATLAB-SIMULINK was used to carry out the control algorithm. Quarc Toolbox connects the Quanser Active Suspension unit to MATLAB. The differences between the active and passive suspension were tested by the equipment in the simulation system.

Key Words: Quarter Car, Active Suspension System, Skyhook, Groundhook, Quanser, LQR.

## KISA ÖZET

### LQR, GROUNDHOOK VE SKYHOOK KONTROL YÖNTEMLERİ KULLANARAK AKTİF SÜSPANSİYONUN TEORİK VE DENEYSEL ANALİZLERİ

Süspansiyon sistemleri, araçları yoldaki rahatsızlıklarından izole etmeye yarar ve araçlardaki titreşimlerin sönümlenmesini sağlar. Bu sistemde tekerlek, aks ve araç gövdesi birbirine bağlanır. Bir aracın lastikleri ile yol arasında sürekli teması sağlamak gerekmektedir. Araçların süspansiyon sistemleri, daha fazla konfor ve güvenlik için geliştirilmiş ve üretilmiştir. Bu noktada sürüş konforu için pasif süspansiyonlar ve yol tutuş yetersiz kalmaktadır. Özellikle elektronik ve bilgisayar teknolojisindeki gelişmeler ve kontrol alanındaki çalışmalar araçlardaki güvenlik, performans ve konfor bileşenlerini içeren sistemlerin geliştirilmesinde ve optimizasyonunda kilit rol oynamıştır. Bu önemli sistemlerden biri araç süspansiyon sistemleridir. Önerilen bu araştırmanın amacı, aktif süspansiyon kontrolü için lineer kvadratik regülatör (LQR), Skyhook ve Groundhook algoritmasını tasarlamak ve uygulamaktır. Araştırmanın amacına yönelik Quanser aktif süspansiyon deney cihazının çeyrek araç modeli kullanılarak LQR, skyhook ve groundhook kontrollü aktif süspansiyon sistemlerinin performansları karşılaştırılmıştır. Bu çalışmada, MATLAB-SIMULINK kontrol algoritmasını yürütmek için kullanılmıştır. Quarc Toolbox, Quanser Aktif Süspansiyon ünitesini MATLAB'a bağlar. Açık ve kapalı süspansiyon arasındaki fark, döngü simülasyon sistemindeki donanım tarafından test edilir.

Anahtar Kelimeler: Çeyrek Araç Modeli, Aktif Süspansiyon Sistemi, skyhook, groundhook, Quanser, LQR.

To my wife and son

## ACKNOWLEDGMENT

In particular, I would like to thank endlessly my respectable thesis advisor Asst. Prof. Dr. Başar ÖZKAN who helped me with his knowledge and experience in every stage of this thesis.

I would like to thank Asst. Prof. Dr. Mümin Tolga EMİRLER for his knowledge and continuous help during my studies.

I would like to thank Mechanical Engineer Fevzi SANIMER for his motivation during my studies.

I would like to thank the Faculty Members at Okan University for their guidance and motivation during my study. Finally, I also thank my family and friends for supporting me during this time.

# TABLE OF CONTENTS

I. INTRODUCTION .....	1
1.1. LITERATURE RESEARCH.....	1
1.2. DEFINITION OF SUSPENSION SYSTEM .....	2
1.3. BASIC SUSPENSION MOVEMENT.....	3
1.4. CLASSIFICATION OF SUSPENSIONS .....	4
II. QUANSER ACTIVE SUSPENSION SYSTEM.....	9
2.1. INTRODUCTION TO THE QUANSER ACTIVE SUSPENSION.....	9
2.2. DESCRIPTION OF QUANSER ACTIVE SUSPENSION COMPONENTS .....	16
2.2.1. Active Suspension DC Motor .....	16
2.2.2. Road Simulation Brushed Servo Motor.....	16
2.2.3. The lead screw .....	17
2.2.4. Middle Plate Encoder.....	17
2.2.5. Suspension Encoder .....	18
2.2.6. Bottom Plate Encoder .....	18
2.2.7. Springs .....	19
2.2.8. Accelerometer .....	20
2.2.9. AMPAQ Power Module .....	20
2.3. ACTIVE SUSPENSION MODEL PARAMETERS .....	22
2.4. COMMUNICATION WITH COMPUTER AND PROGRAMS .....	24
2.4.1. Matlab .....	24
2.4.2. Quarc.....	24
III. MODELLING OF SUSPENSION SYSTEM.....	25
3.1. QUARTER CAR MODEL OF THE ACTIVE SUSPENSION .....	25
3.2. STATE SPACE REPRESENTATION .....	30
3.3. SYSTEM TRANSFER FUNCTIONS .....	32
IV. CONTROL DESIGN OF ACTIVE SUSPENSION SYSTEM.....	33
4.1. INTRODUCTION.....	33

V. CONTROL METHODS .....	38
5.1. CONTROLLABILITY AND OBSERVABILITY .....	38
5.2. IMPLEMENTING OF CONTROL METHODS .....	38
5.3. LINEAR QUADRATIC REGULATOR (LQR) CONTROL .....	42
5.3.1. Performance Studies of LQR Control Method .....	45
5.4. SKYHOOK CONTROL .....	52
5.4.1. Performance Studies of Skyhook Control Method .....	53
5.5. GROUNDHOOK CONTROL.....	57
5.5.1. Performance Studies of Groundhook Control Method .....	58
VI. IMPLEMENTATION AND EXPERIMENTAL RESULTS .....	62
VII. CONCLUSIONS AND RECOMMENDATIONS.....	75
APPENDIX.....	79
VITA.....	81



## LIST OF TABLES

Table I-1. Suspension Systems .....	7
Table II-1. List of parts of Quanser Active Suspension.....	12
Table II-2. Brushed Servo Motor Characteristics .....	17
Table II-3. Active Suspension Spring Characteristics. ....	19
Table II-4. AMPAQ Specifications. ....	22
Table II-5. Active Suspension System Parameters.....	23
Table V-1. Weighting coefficients in LQR design. ....	46
Table V-2. Coefficients in Skyhook design.....	53
Table V-3. Coefficients in Groundhook design.....	58

## LIST OF FIGURES

Figure I-1. Vehicle axis system .....	3
Figure II-1. Quanser Suspension Plant. ....	10
Figure II-2. Top Plate of Quanser Active Suspension System .....	14
Figure II-3. System Inputs .....	14
Figure II-4. Middle Plate Side View of Quanser Active Suspension .....	15
Figure II-5. Bottom front View of Quanser Active Suspension System .....	15
Figure II-6. Bottom back View of Quanser Active Suspension System.....	16
Figure II-7. Encoder Connection Diagram .....	18
Figure II-8. Quanser AMPAQ with the wired cables. ....	21
Figure III-1. Quarter Car Model of Active Suspension System .....	25
Figure III-2. Free-body Diagram of Sprung Mass .....	26
Figure III-3. Free-body Diagram of Unsprung Mass.....	27
Figure IV-1. Active Quarter Car Suspension Model . ....	34
Figure IV-2. Simulink diagram of active suspension system .....	37
Figure V-1. Active Suspension Plant Simulink Blocks .....	39
Figure V-2. Road Surface Generator Block.....	40
Figure V-3. Road Simulator Block .....	40
Figure V-4. Vehicle Body Block .....	41
Figure V-5. Suspension Block .....	41
Figure V-6. Control Actuator Block .....	42
Figure V-7. Vertical acceleration of vehicle body.....	46
Figure V-8. Tire Deflection .....	47

Figure V-9. Vertical acceleration of vehicle body.....	48
Figure V-10. Tire Deflection .....	48
Figure V-11. Vertical acceleration of vehicle body.....	49
Figure V-12. Tire Deflection .....	50
Figure V-13. Vertical acceleration of vehicle body.....	51
Figure V-14. Tire Deflection .....	51
Figure V-15. Structure of skyhook control .....	53
Figure V-16. Sprung mass acceleration for $c_{sky}=1000$ .....	54
Figure V-17. Tire deflection for $c_{sky}=1000$ .....	54
Figure V-18. Sprung mass acceleration for $c_{sky}=10000$ .....	55
Figure V-19. Tire deflection for $c_{sky}=10000$ .....	55
Figure V-20. Sprung mass acceleration for $c_{sky}=100000$ .....	56
Figure V-21. Tire deflection for $c_{sky}=100000$ .....	56
Figure V-22. Structure of Groundhook control .....	57
Figure V-23. Tire deflection for $c_{gnd}=100$ .....	58
Figure V-24. Sprung mass acceleration for $c_{gnd}=100$ .....	59
Figure V-25. Tire deflection for $c_{gnd}=1000$ .....	59
Figure V-26. Sprung mass acceleration for $c_{gnd}=1000$ .....	60
Figure V-27. Tire deflection for $c_{gnd}=10000$ .....	60
Figure V-28. Sprung mass acceleration for $c_{gnd}=10000$ .....	61
Figure VI-1. Sprung mass acceleration with square wave signal test1 .....	62
Figure VI-2. Sprung mass acceleration with square wave signal test <sub>2</sub> .....	63
Figure VI-3. Tire Deflection with square wave signal test <sub>2</sub> .....	63
Figure VI-4. Sprung mass acceleration with square wave signal test <sub>3</sub> .....	64

Figure VI-5. Tire Deflection with square wave signal test <sub>3</sub> .....	64
Figure VI-6. Sprung mass acceleration with square wave signal test <sub>4</sub> .....	65
Figure VI-7. Tire Deflection with square wave signal test <sub>4</sub> .....	65
Figure VI-8. Sprung mass acceleration with random signal test <sub>2</sub> .....	66
Figure VI-9. Tire Deflection with random signal test <sub>2</sub> .....	66
Figure VI-10. Sprung mass acceleration with random signal test <sub>3</sub> .....	67
Figure VI-11. Tire Deflection with random signal test <sub>3</sub> .....	67
Figure VI-12. Sprung mass acceleration with random signal test <sub>4</sub> .....	68
Figure VI-13. Tire Deflection with random signal test <sub>4</sub> .....	68
Figure VI-14. Sprung mass acceleration with random signal c <sub>sky</sub> =100 .....	69
Figure VI-15. Tire Deflection with random signal c <sub>sky</sub> =100 .....	69
Figure VI-16. Sprung mass acceleration with square wave signal c <sub>sky</sub> =100.....	70
Figure VI-17. Tire Deflection with square wave signal c <sub>sky</sub> =100.....	70
Figure VI-18. Sprung mass acceleration with square wave signal c <sub>gnd</sub> =100 .....	71
Figure VI-19. Tire Deflection with square wave signal c <sub>gnd</sub> =100 .....	71
Figure VI-20. Sprung mass acceleration with random signal c <sub>gnd</sub> =100.....	72
Figure VI-21. Tire Deflection with random signal c <sub>gnd</sub> =100 .....	72
Figure VI-22. Sprung mass acceleration with random signal.....	73
Figure VI-23. Tire Deflection with random signal c <sub>gnd</sub> =100 and c <sub>sky</sub> =100.....	73
Figure VI-24. Sprung mass acceleration with square wave signal .....	74
Figure VI-25. Tire Deflection with square wave signal .....	74

## SYMBOLS

$m_s$	Mass of Vehicle Body
$m_u$	Mass of Suspension
$k_s$	Spring Coefficient of Suspension
$k_t$	Spring Coefficient of Tire
$b_s$	Damper Coefficient of Suspension
$b_t$	Damper Coefficient of Tire
$N$	Newton
$F_c$	Control Force
$z_t$	Position of Tire
$z_s$	Position of Vehicle Body
$z_u$	Position of Suspension
$J$	Transition Matrix
$\omega_{\text{resonance}}$	Resonant Frequency of Suspension

## ABBREVIATIONS

- EOM** : Equations of Motion
- LQR** : Linear Quadratic Regulator
- PID** : Proportional Integral Derivative
- DC** : Direct Current
- MIMO** : Multi-Input Multi-Output
- ID** : Identification Number

# I. INTRODUCTION

In this section, firstly, general information about the subjects determining the thesis study is given. Then, the importance of the thesis topic is mentioned. Previous researches have been put forward. In this study, the results of the literature survey about the subjects are given in the related sections. Finally, in the scope of the thesis, what is explained in the sections that constitute the content of the thesis is given in general.

## 1.1. Literature Research

Active suspension systems can be examined in two groups. The first one is fully active systems and the other is slow active systems.

In fully active systems, the vehicle suspension has a very advanced dynamic behaviour. An electromagnetic linear motor operates parallel to the springs in this system. This motor controls the system by applying a control force for damping. The actuator, which can be an electromotor or hydraulic cylinder, can adjust the spring assembly to form the desired system for each wheel in slow active suspension. This system reduces rolling movements of the vehicle.

We can show the suspension system control in vehicles in two groups as linear and non-linear. Examples of linear control methods include PID control, Skyhook control, Groundhook control,  $H_\infty$  control and LQR method [1]. Nonlinear systems are generally obtained according to Lyapunov's theorems [2]. In the study conducted by Foda, fuzzy logic and PID controller were compared for quarter vehicle active suspension system and fuzzy logic controller was superior [3]. In the study conducted by Gysen and his friends, forward and reverse feed control was performed for a different electromagnetic active suspension system. According to this study, good

reference tracking is provided for driving comfort and safety [4]. In the study conducted by Van der Sande et al., A robust  $H_{\infty}$  dynamic output feedback control was designed for the control of active suspension system and a comfort increase of approximately 40% was achieved [5]. In the study conducted by Fateh and his friends, the impedance of the hydraulic system in the suspension system was controlled [6]. A successful formula for passenger comfort and driving safety has been developed and successful results have been presented with respect to passive suspension. Emura and colleagues in their work with the vehicle body of the ideal skyhook suspension damper suspended at the same speed moving the air suspension system with the help of a virtual damper modelled [7].

In practice, the skyhook damper must be mounted between the wheel and the vehicle body assembly since it is not possible to be connected an airborne point. The required damping force is also applied by this new damper.

Ahmadian also mentioned groundhook suspension control, which isolates the wheel assembly from road influences. Groundhook Suspension control is in principle similar to skyhook control. Alternatively, the damper is connected to a virtual reference point on the ground surface, not the air [8]. In the study conducted by Agharkakli and his friends the active suspension system LQR controller was designed with the ready MATLAB `lqr` command [9].

## **1.2. Definition of Suspension System**

Suspension is the system consisting of springs, dampers and other components providing the movement between the vehicle and the wheels by connecting the body of a vehicle to the wheels. In short, all the parts connecting the wheels to the vehicle are called the suspension system.



Suspension systems are designed to provide good road holding and improve ride comfort. Passengers inside the vehicle are not disturbed by road noise and vibrations in the vehicle. Therefore, the suspension must be properly adjusted. One of the most important tasks of the suspension is the contact of the wheel with the road surface. Many forces act on the vehicle to reduce wheel contact with the road. Accidents can occur as a result of reduced tire contact with the road surface. Due to the good suspension system, it is protected in the transported goods inside the vehicle. It may show differences in the front and rear side of the suspensions in vehicles [10].

### 1.3. Basic Suspension Movement

A vehicle in motion is affected by a lot of forces due to bad road and adverse weather conditions. These forces cause some oscillations in the vehicle as shown in Figure I-1.

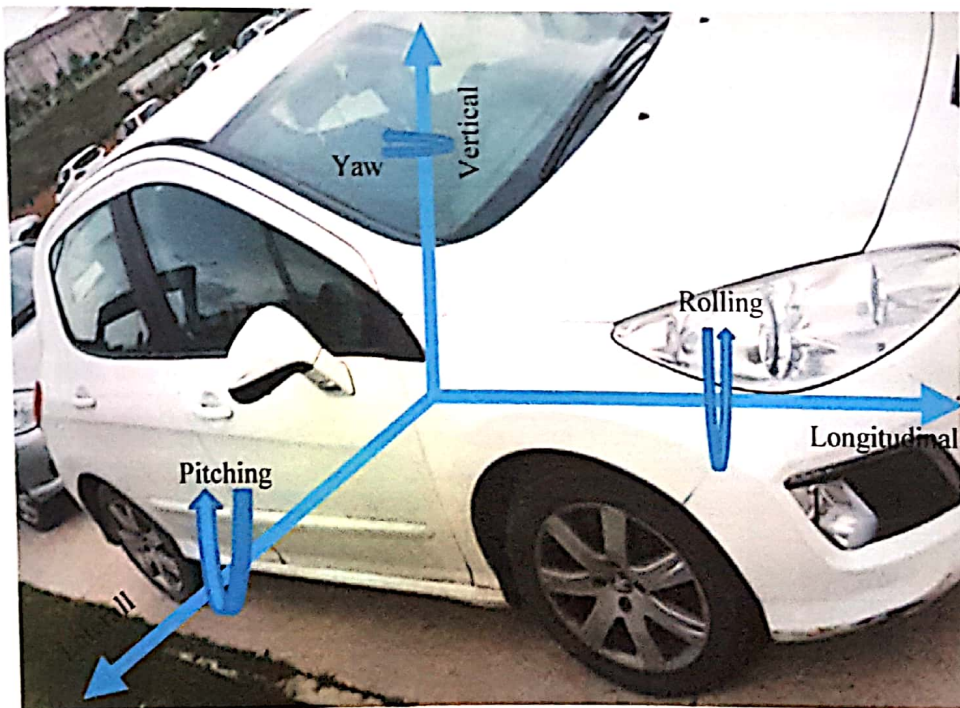


Figure I-1. Vehicle axis system

The movement around the longitudinal axis is called Rolling. When the vehicle is turning or moving on a broken road, the spring on one side of the vehicle shortens while the other begins to grow. As a result, the body of the vehicle makes lateral movements from one side to the other.

The movement around the vertical axis is called yaw. It is a completely up and down movement of the vehicle. It occurs when the vehicle is driven at high speeds on rough roads.

The movement around the lateral axis is called pitching. The front and the back of the vehicle is moving up and down according to the centre of gravity. This jerking occurs in particular when the vehicle is used on rough and pot-holed roads [1].

#### **1.4. Classification of Suspensions**

A normal car suspension consists mainly of a spring and a shock absorber. When the spring is selected solely on the weight of the vehicle, the damper must isolate the passengers from low-frequency road disturbances and absorb high-frequency road disturbances.

As the suspensions carry the vehicle body, they transmit all the forces coming from the road into the vehicle. The damping coefficients for the spring and shock absorbers are selected according to the vehicle's handling and driving comfort. Only these selected coefficients can produce a balance between the driving comfort and the handling of the vehicle. However, it cannot be adjusted according to all kinds of road conditions. With the development of microprocessors and sensors starting from the 80s, works for the production of intelligent suspensions began. With the advancement of the actuator technology, the state of the springs and shock absorbers can be controlled according to

the road conditions. Intelligent suspension systems can be classified into two main groups. These are semi active and fully active suspension systems respectively.

Since active suspensions generate force according to the road condition, energy usage is also high. This is achieved by the force exerted by the actuators. Totally active suspension is much better in terms of driving comfort than passive and semi active suspension, but it is limited because it is an expensive system. In 1982 Lotus car designed active suspension for Formula 1 vehicles. But then this prototype active suspension was banned.

In 1987, Mitsubishi developed the first electronically controlled semi active suspension system in the world and used this system in the Mitsubishi Galant model. This system with low energy requirements in the following years, the trademarks like Audi, Ferrari, Chevrolet has been applied to some models. the 90s, Nissan increased the price of its luxury vehicles by twenty percent and optionally included active suspension in these vehicles. However, this Active suspension system was operating in the low band range.

In conventional mechanical and semi-mechanical suspension systems with hydraulic and pneumatic shock absorbers, the tire reacts instantly to the vehicle when it touches a different surface.

Even if most of this message is damped by the suspension system, some of it is transmitted to the vehicle. This causes jerking in the bend and the vehicle to lie in bends. Recently, fully active suspensions produced by Bose Corporation use DC motors instead of hydraulic or pneumatic actuators. Electromagnetic motors on each wheel independently operate on electric power These engines were powered by amps and the vehicle was constantly under control. The entire weight of the vehicle was under

suspension control during bumps and turns, so the system officially resisted the rules of physics. The Bose active suspension system is controlled by a brain and each electromagnetic motor can be intervened separately. In this way, each suspension is evaluated according to the ground conditions.

The control computer checks the state of each suspension in milliseconds, which allows the tire to adapt to the different ground as soon as it touches the tire. Comparisons on the advantages and disadvantages of Yue et al., determining criteria for comparison of passive suspension semi active suspension and fully active suspension are shown in Table I-1.

Control engineers are involved in an intelligent suspension design. In order to improve driving comfort and good road holding, it is necessary to first model the vehicle's dynamic model. Then, it is necessary to select and design adjustments in control strategies to balance driving comfort and handling.

Table I-1. Suspension Systems

Parameters	Passive Suspension	Semi active Suspension	Electromagnetic Active Suspension	Hydraulic or pneumatic active suspension
<b>Structure</b>	Simplest	Complex	Simple	Most complex
<b>Weight or Volume</b>	Lowest	Low	Highest	High
<b>Cost</b>	Lowest	Low	Highest	High
<b>Ride Comfort</b>	Bad	Medium	Best	Good
<b>Handling performance</b>	Bad	Medium	Best	Good
<b>Energy regeneration</b>	No	No	Yes	Medium
<b>Reliability</b>	Highest	High	High	Medium
<b>Dynamic performance</b>	Passive	Passive	Good	No
<b>Commercial Maturity</b>	Yes	Yes	No	Yes

The dynamic model of intelligent vehicle suspensions is very important. It is necessary to design a model that is very close to the real vehicle. Thus, the controller must provide good performance in real-time control. The mass of the vehicle body varies in most vehicles. The mass of the vehicle will vary depending on the number of passengers boarded or the load it carries. Therefore, determining the vehicle body mass in the vehicle's dynamic model will not be sufficient to determine the vehicle's dynamic behaviour.

Sensors, controllers and actuators in intelligent suspension systems are in a closed circuit. Time may be delayed during measurements. This time delay is often neglected because it is a very small value. Time delay in active suspensions may cause the vehicle

to become unstable. There is not energy input in the semi-active suspensions. Therefore, there is no stability problem in the vehicle.

The decrease in the performance of the semi active suspension results from a time delay. The active suspension components are affected over time by road conditions. Faults in these components should be dealt with in a timely manner. Otherwise, the vehicle loses its stability and cannot achieve the desired performance with active suspension [15].

## II. QUANSER ACTIVE SUSPENSION SYSTEM

### 2.1. Introduction to the Quanser Active Suspension

Quanser Active Suspension is a test device which is used in the quarter car model. The model of the Quanser Suspension test device is shown in the Figure II-1. The plant has three overlapping plates. The top Plate represents the vehicle body. This plate is connected with two springs and placed on the middle plate. An Accelerometer for measuring the acceleration of the Vehicle Body is hung on this plate [12].

A high performance DC motor is placed between the middle and top plates to simulate a semi active or active suspension mechanism. The wheel of the vehicle is represented the middle plates. The middle plate is hung on the bottom plate with two springs.

The bottom plate represents the bottom plate. This plate connects to another quick-response DC Motor which enables it to produce different road profiles.

These three plates can slide linearly along a stainless shaft. When the DC motor rotates, a torque is generated on the output shaft. This torque is converted to a linear force that causes the bottom plate to move along the lead screw. High resolution optical encoders in the centre monitor the movements of the top plate while other encoders measure the movement of the bottom plate. To investigate active control algorithms was used this quarter car structure.

The purpose of the active suspension experiment is to design and implement an observer-based state feedback controller for a quarter-car model. In this system, there are two masses supported by spring and shock absorber. One of these masses  $m_s$  represents the mass of the vehicle body. The other mass  $m_u$  represents the wheel mass.

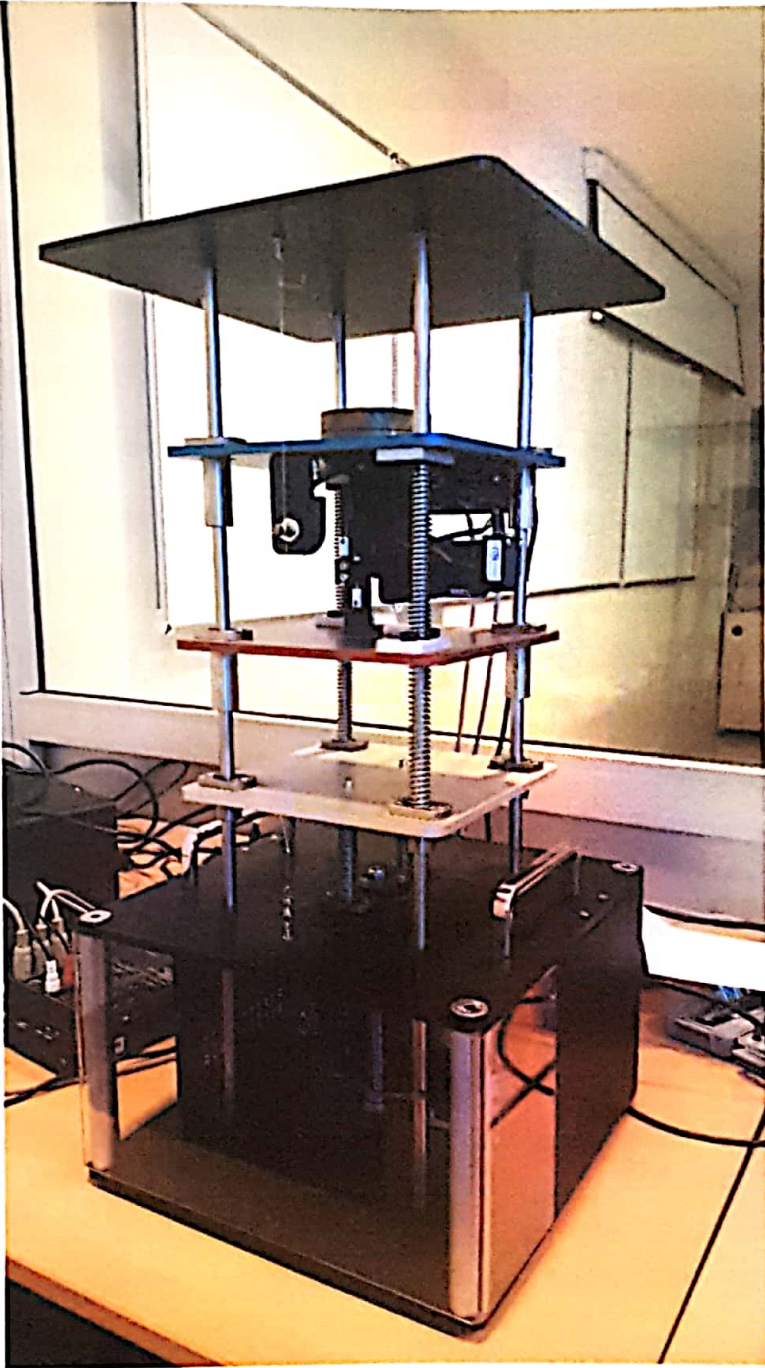


Figure II-1. Quanser Suspension Plant.



The suspension spring coefficient  $k_s$  represents the stiffness of the springs physically used in the suspension. Since the  $k_s$  value of the suspension springs cannot change after production, they are manufactured with certain performance criteria in mind during production. Suspension damper coefficient  $b_s$  represents the stiffness of dampers or dampers physically used in the suspension. Since the  $b_s$  value of the suspension dampers cannot change after production, they are manufactured with certain performance criteria in mind during production. The wheel spring coefficient  $k_t$  physically represents the stiffness of the wheel. The tire coefficient  $b_t$  represents the stiffness of damper in the tire. The shock absorber constant in the wheel is very low, which is often neglected. The LQG control optimizes a variety of performance parameters in a quarter-car model. In this approach, the performance criteria are formulated into a mathematical model. This mathematical representation is then optimized while considering the control actuator limitations. The performance measures that have to be minimized are listed below.

- Avoiding unwanted forces from the road is often referred to as ride quality. When measuring the ride quality, vertical acceleration of the vehicle can be considered as a performance parameter. A good suspension system should minimize the acceleration ( $\ddot{z}_s$ ) of the unsprung mass, that is the vehicle body consisting of jolts on the road.

- The suspension system assists in the static load stability of the vehicle, usually on curved roads and bends. This property is related to the impact of the suspension; It facilitates the rotation by providing the transfer of weight from the high side to the low side of the vehicle at turns. This weight transfer can also be measured by minimizing the suspension deflection ( $z_s - z_u$ ) mentioned.

● The criteria for road handling are basically the ability of the vehicle to turn and to brake. These criteria can be achieved in order to be very good performance by minimizing the amount of load on the wheels. This is because all the horizontal and vertical forces generated by the wheel are directly linked to the wheel load. Thus, the road handling of vehicle is directly related to the deflection that occurs in the vertical direction and can be defined as  $z_u - z_f$  [12].

The table II-1. containing all components of the Quanser active suspension system is given below. The components of the Quanser Active Suspension test device in Figure II-1. have an identification number (ID). These are as shown in Figure II-2., Figure II-3., Figure II-4., Figure II-5. and Figure II-6

Table II-1. List of parts of Quanser Active Suspension

ID#	Definition	ID#	Definition
1	Top Plate (Blue, Mass of Vehicle Body)	2	Accelerometer Gain Potentiometer
3	Middle Plate (Red, Mass of Vehicle Tire )	4	Suspension Encoder
5	Bottom Plate (white, Road)	6	Suspension Motor Capstan Cable
7	2 Adjustable Springs (Springs of Vehicle Suspension)	8	Spring Holder Set Screw
9	2 Adjustable Springs (Vehicle Tire Spring)	10	Linear Bearing Blocks
11	Bottom Plate Encoder Connector	12	Top Plate Encoder Connector

13	Bottom Plate Counter Weight Springs	14	Payload Mass
15	Active Suspension DC Motor	16	Bottom Plate Encoder
17	Bottom Plate Servo Motor	18	Lead Screw
19	Encoder Thread	20	Stainless Steel Shafts
21	Accelerometer	22	Accelerometer Connector
23	Plant Top Cover	24	Limit Switch Safety Lights
25	Plant Handles	26	Bottom Plate Motor Connector
27	Limit Switch Push Key	28	Safety Rod
29	Movable Spring Holders	30	Safety Limit Switch
31	Suspension Motor Connector	32	Suspension Encoder Connector
33	Encoder Thread Anchor	34	Top Plate Encoder

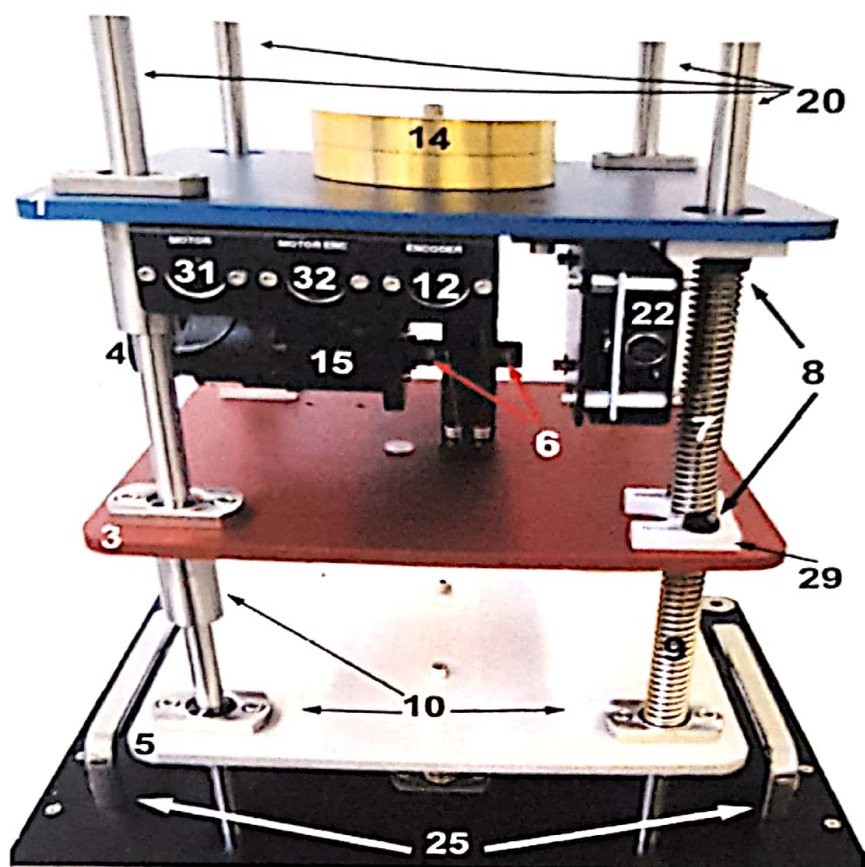


Figure II-2. Top Plate of Quanser Active Suspension System



Figure II-3. System Inputs

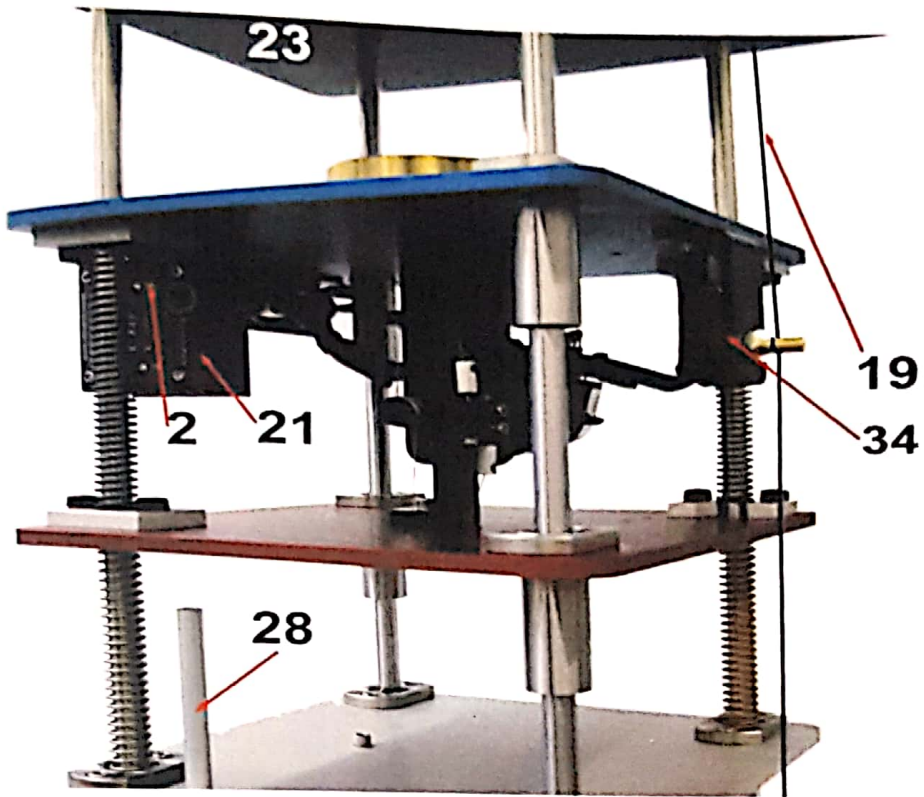


Figure II-4. Middle Plate Side View of Quanser Active Suspension

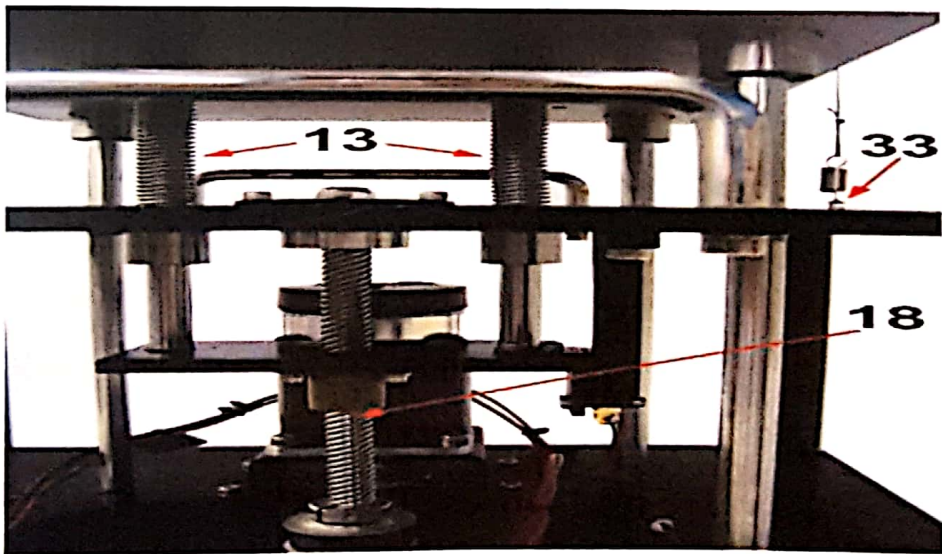


Figure II-5. Bottom front View of Quanser Active Suspension System

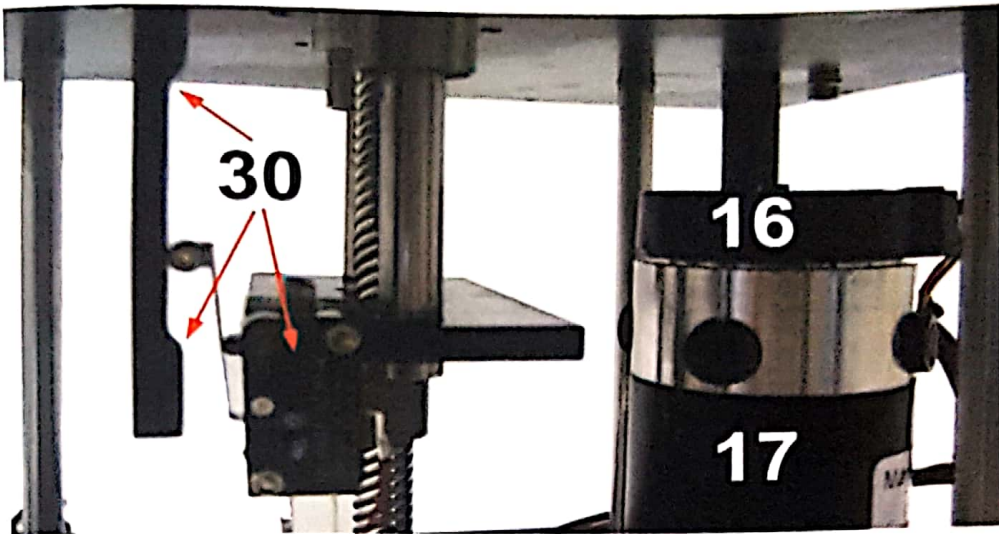


Figure II-6. Bottom back View of Quanser Active Suspension System

## 2.2. Description of Quanser Active Suspension Components

### 2.2.1. Active Suspension DC Motor

The Quanser Active Suspension test device includes a Faulhaber Coreless DC Motor (3863V006), as represented in Figure II-2. by component #15. This DC motor model is a high efficiency low inductance motor resulting in a much faster response than a classic DC motor [12].

### 2.2.2. Road Simulation Brushed Servo Motor

The Quanser Active Suspension Device includes a Magmotor Brushed Servo Motor, as shown in Figure II-6. by ID #17. The motor has a power of 70 Watts. The motor is connected to the lead screw through the geared pinion and cable transmission. The lead screw converts the rotational motions of the motor into the linear motions of the bottom plate. Some of the motor characteristics are included in Table II-2. [12].

Table II-2.Brushed Servo Motor Characteristics [12].

Frame Size	Stack Length	Peak Stall Torque	Cont. Stall Torque	Rotor Inertia	Friction Torque	Thermal Resistance (Rm) Oc/Watt	Max Recommended Speed Rpm	Max Winding Temperature (C)	Power Range (W)	Weight (lb)
S23	100	500	50	0.006	5	4.5	4000	155	70	2

### 2.2.3. The lead screw

The lead screw, shown by ID #18 in Figure II-5. circulates through a ball nut, that is attached to the bottom of the bottom plate and is rotated by the motor. The lead screw has a pitch of 1.27 cm. Thus the road simulation plate moves 1.27 cm, per single ball-screw revolution [12].

### 2.2.4. Middle Plate Encoder

Digital position measurement of middle plate vertical motion is obtained by using a high-resolution quadrature optical encoder. The encoder has a resolution of 1024 lines per revolution. In quadrature mode this gives 4096 counts per full rotation of the encoder shaft. The effective resolution, i.e. minimum linear position that can be detected, of the stage displacement is  $4.87 \mu\text{m}$ .

The inertial wiring diagram of the encoder is depicted in Figure II.5. The encoder standard 5-pin DIN connector, shown in Figure II-2, is also pictured as component #12.

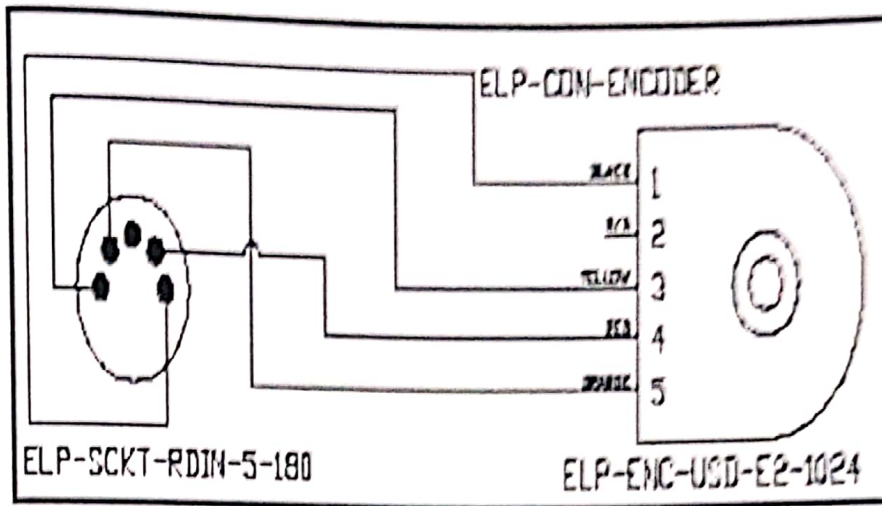


Figure II-7. Encoder Connection Diagram [12]

### 2.2.5. Suspension Encoder

The high-resolution digital optical encoder performs digital measurement of the movement of the suspension. This optical encoder is mounted on the behind of the active suspension DC motor. The motor encoder has a resolution of 1000 lines per revolution. In quadrature mode this gives 4000 counts per full rotation of the encoder shaft. The effective resolution, i.e. minimum linear position that can be detected, of the stage displacement is  $9.42 \mu\text{m}$ .

The encoder standard 5-pin DIN connector is pictured as component #4 in Figure II-2. Pushing the middle plate and top plate towards each other should result in negative change of encoder reading.

### 2.2.6. Bottom Plate Encoder

The high-resolution digital optical encoder performs digital measurement of the movement of the bottom plate. This optical encoder is mounted on the behind of the brushed servo motor of active suspension. Digital position measurement of bottom plate



is obtained by using a high-resolution quadrature optical encoder. The optical encoder is directly mounted on the rear of the brushed servo motor. The motor encoder has a resolution of 2048 lines per revolution. In quadrature mode this gives 4096 counts per full rotation of the encoder shaft. The effective resolution i.e. minimum linear position that can be detected, of the stage displacement is  $2.19 \mu\text{m}$ .

The encoder standard 5-pin DIN connector is pictured as component #16 in Figure II-6. Pushing the bottom plate upwards should result in positive change of encoder reading.

### 2.2.7. Springs

The following sets of springs are supplied with Active Suspension Plant as shown in Table II.3. Moreover, two springs are installed on the device upon delivery. These springs are used to compensate for the weight of the three moving plates and reducing the pressure on the servo motor.

Table II-3.Active Suspension Spring Characteristics.

Name	Application	Length	Quantity	Color	Stiffness per spring
FUF-14 128-A	Suspension	0.128m	2	Black(installed upon delivery)	490N/m
FUF-14 128-B	Suspension	0.128m	2	Orange	1020N/m
FUF-14 115-A	Tire	0.115m	2	Black	570N/m
FUF-14 115-B	Tire	0.115m	2	Orange(installed upon delivery)	1250N/m

### 2.2.8. Accelerometer

To measure the vertical acceleration of the vehicle body, there is a biaxial ADXL210E accelerometer under the top blue plate. It is shown with ID #21 label in Figure II-4.

The accelerometer has the capability to measure both AC/dynamic acceleration (e.g. vibrations) and DC/static accelerations (e.g. gravity). The arrows represented on the accelerometer, and depicted in Figure II.4, show the positive direction of the AC acceleration sensor measurement on its axes of sensitivity. To best measure the Active Suspension top plate (vehicle body) vibration, the accelerometer is mounted such that its x-axis is longitudinal to vertical direction. Quickly pushing the top plate (component #1) upwards should result in an initial negative measured acceleration voltage. In order for the accelerometer reading to be consistent with the encoder measurements its sign should be negated in the control software.

The sensor has a range of  $\pm 10$  g and its noise, in the operating range of the top plate, is approximately  $\pm 5.0$  mV, i.e.  $\pm 5.0$  mg. This analog sensor is calibrated such that 1 Volt equals 1 g, or  $9.81$  m/s<sup>2</sup>. Although the Active Suspension accelerometer has already been calibrated at the factory, the signal conditioning circuit properties may vary depending on the external conditions (e.g. humidity, temperature). Therefore, you may want to adjust the Offset potentiometer (shown as component #2 in Figure II.2) such that it reads approximately zero Volts with zero acceleration (i.e. sensor resting flat/horizontally) [12].

### 2.2.9. AMPAQ Power Module

The AMPAQ Power Module, shown in Figure II-8., is a pulse-width modulated current amplifier. It is used to drive the two motors of Active Suspension Plant. The

power module's specifications are given in Table II-4. The signals from the data-acquisition board are to be connected to the Input connector. The Sense connector outputs the current measured in the attached motors. The Enable connector socket of AMPAQ receives digital input signals from the PC in order to enable or disable the power module. Finally, the amplified current is sent from the Output connector

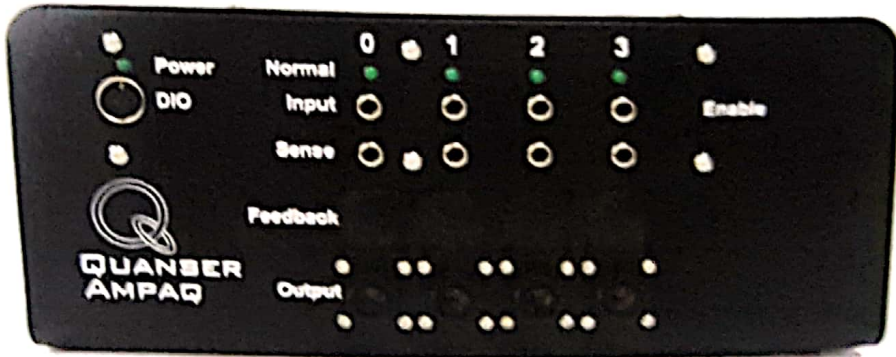


Figure II-8. Quanser AMPAQ with the wired cables.

Each motor-driving amplified current signal from each Output socket of the AMPAQ has its own indicator LED. When a particular Output signal is enabled, such that its corresponding motor, to which it is connected, can be actuated, then its corresponding LED lights up. When a particular Output signal is disabled, that is its connected motor cannot be actuated, then its corresponding LED stays off. For example, if the AMPAQ's Output #2 is enabled, then a motor that is connected to the Output 2 socket will be actuated; furthermore, the Normal #2 LED will become lit. If, however, Output #2 is disabled, then LED 2 will not light up, and the corresponding motor to Output #2 socket will not be actuated.

Table II-4. AMPAQ Specifications.

Symbol	Description	Value	Unit
	AMPAQ Maximum Input Voltage Range Note: This value is for reference only; particular control signal levels will result in unique voltage input levels.		
	AMPAQ Maximum Input Current Note: This value is for reference only; particular loading will result in unique electrical current use.	25	mA
	AMPAQ Enable Ribbon Cable Signal's Voltage Range	0 to 5	V
	AMPAQ Enable Ribbon Cable Signal's Electrical Current (Absolute Maximum Value)	1	mA
	External Power Source RMS Voltage Required to Operate AMPAQ	120/240	V
	External Power Source Voltage Frequency Required to Operate AMPAQ	60/50	Hz
<b>VA_SUP</b>	AMPAQ Supply Voltage	27	V
<b>VA_RNG</b>	AMPAQ Voltage Input Range	$\pm 10$	V
<b>Ka</b>	AMPAQ Gain	0.5	A/V
<b>IMAX</b>	AMPAQ Maximum Peak Output Note: This value is for reference only; particular motor resistance and loading will result in unique electrical current sourcing levels	7	A
<b>IMAX, CONT</b>	AMPAQ Continuous Output Current	2.15	A
<b>B</b>	Current Amplifier Bandwidth	500	Hz

### 2.3. Active Suspension Model Parameters

Table II.5. below lists and characterizes the main parameters (e.g. mechanical and electrical specifications, conversion factors) associated with the Active Suspension System. Some of these parameters can be used for mathematical modelling of the plant as well as to obtain the system Equations of Motion (EOM). [12]

Table II-5. Active Suspension System Parameters.

Symbol	Description	Value	Unit
	Structure Total Weight	15.00	kg
$m_t$	Top Plate with Attached Equipment Total Mass	2.45	kg
$m_m$	Middle Plate(Red) with Attached Equipment Total Mass	1.00	kg
$k_s$	Linear Stiffness Constant of Passive Suspension	900	N/m
$k_t$	Linear Stiffness Constant of Tire	250	N/m
$b_s$	Damping Constant of Suspension	7.5	N.s/m
$b_t$	Damping Constant of Tire	5	N.s/m
	Torque Constant of Suspension Motor	0.115	N.m/A
	Shaft Radius Of Suspension Motor	0.006	m
	Suspension Encoder Resolution	942e-6	m/count
	Bottom Plate Encoder Resolution	219e-6	m/count
	Middle Plate Encoder Resolution	487e-6	m/count
	Suspension Travel Range	3.80e-002	m
	Middle Plate Travel Range	3.00e-002	m
	Bottom Plate Travel Range	3.60e-002	m

## **2.4. Communication with computer and Programs**

### **2.4.1. Matlab**

In this thesis, MATLAB is used for applying control algorithms. MATLAB is a high-performance software for technical and scientific calculations, mainly involving numerical calculation, graphical data representation and programming. Typical applications of Matlab are: mathematical and computational operations, algorithm development, modelling, simulation and pre-typing, Data analysis and visual effects supported representation, scientific and engineering graphics, application development [13].

### **2.4.2. Quarc**

Quarc is an integral part of Quanser's lab workstations and the comprehensive courseware with Simulink-based lab exercises that accompany them. QUARC user interfaces are easy to understand. We can work with controllers that are clear and match standard system block diagrams used in textbooks we can tune parameters of the running model by changing block parameters in the Simulink diagram, view the status of a signal in the model and stream data to MATLAB workspace or to a file for off-line analysis [14].

### III. MODELLING OF SUSPENSION SYSTEM

#### 3.1. Quarter Car Model of the Active Suspension

In this section, the active suspension system is considered as a double mass damper system and dynamic equations are obtained. In the quarter car model, the vehicle body and the axle and wheel are represented by sprung mass and unsprung mass corresponding to approximately one quarter car. The dynamic model of a system helps us simulate the real system and test control strategies. The method of free-body diagram is used to obtain the dynamics of the active suspension system as a double mass spring model. In this approach, the two inputs to the system are considered to be control command  $F_c$  and the road surface position  $z_r$ . In The Figure III-1. is shown quarter car Model of active Suspension system.

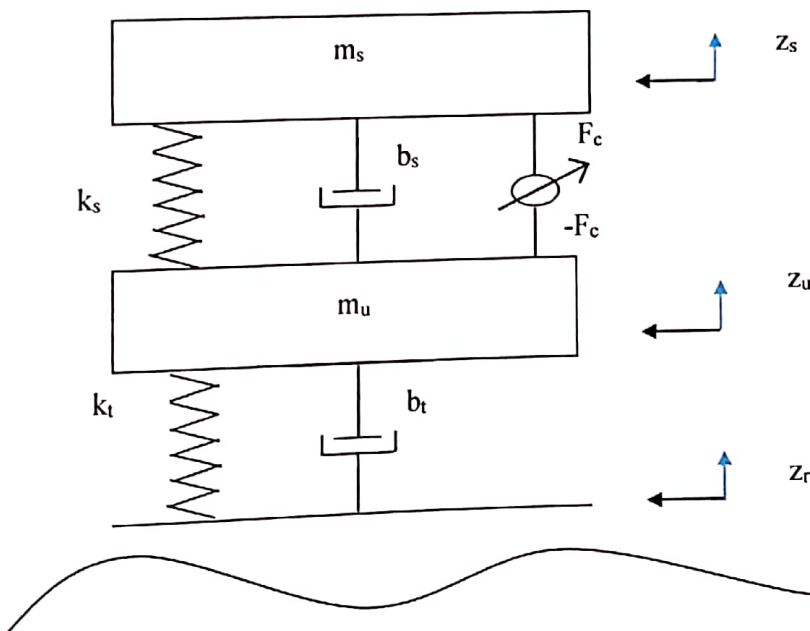


Figure III-1. Quarter Car Model of Active Suspension System

Furthermore, it is reminded that the reference frames in Figure III.1 are used to choose the generalized coordinates, i.e.  $z_s$  and  $z_u$ . The generalized coordinate  $z_u$

represents the tire displacement and  $z_u$  represents vehicle body displacement all with respect to the ground.

To find out equations of motion (EOM) for this system, the free-body diagram for each mass should be determined. There are two masses in the system. The forces applied to each mass should be drawn on the diagrams. we should have two equations of motion. The free-body diagram for  $m_s$  is shown as in the Figure III-2.

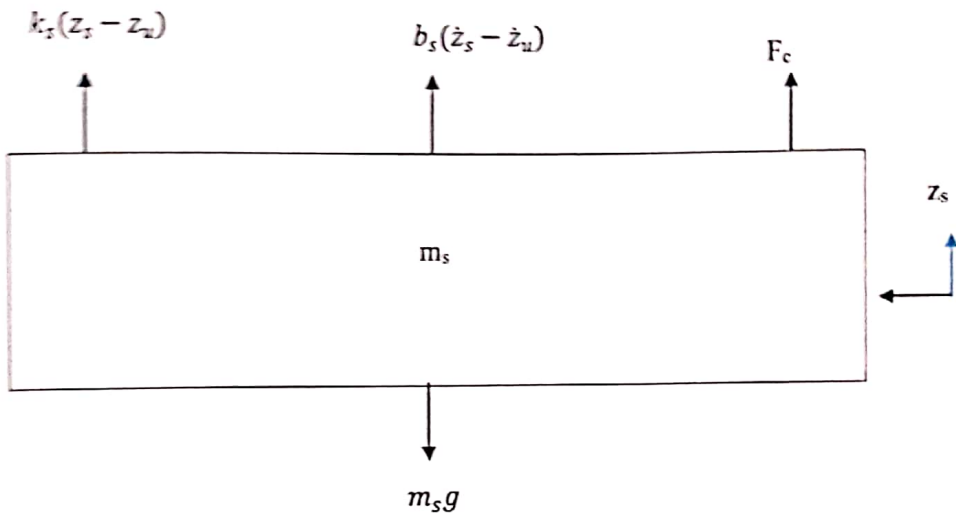


Figure III-2. Free-body Diagram of Sprung Mass

The equation of motion for the model above will be:

$$\frac{d^2}{dt^2} z_s(t) = -g + \frac{F_c}{m_s} + \frac{b_s \left( \frac{d}{dt} z_s \right)}{m_s} - \frac{b_s \left( \frac{d}{dt} z_u \right)}{m_s} + \frac{k_s z_s}{m_s} - \frac{k_s z_u}{m_s} \quad (\text{III.1})$$



The free-body diagram for  $m_u$  will look like the Figure III-3. below:

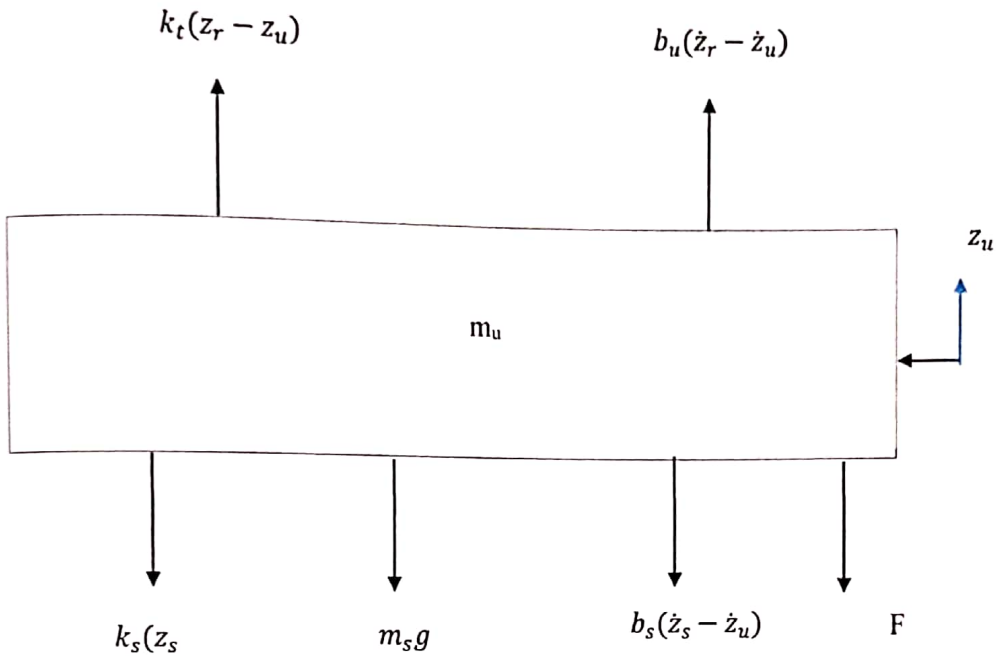


Figure III-3. Free-body Diagram of Unsprung Mass

The equation of motion for the model above will be:

$$\begin{aligned} \frac{d^2}{dt^2} z_u = -g - \frac{F_c}{m_u} + \frac{(-b_s - b_t \left( \frac{d}{dt} z_u \right) + \frac{b_s \left( \frac{d}{dt} z_s(t) \right)}{m_u}}{m_u} \quad (III.2) \\ + \frac{b_t \left( \frac{d}{dt} z_r \right)}{m_u} + \frac{(-k_t - k_s) z_u}{m_u} + \frac{k_s z_s}{m_u} + \frac{k_t z_r}{m_u} \end{aligned}$$

The gravitational force in these equations only changes the equilibrium points for the Active Suspension system and does not affect the dynamics of the system. In our basically derived motion equations, we can set  $g$  to zero and use these equations for the rest of the curriculum. The generalized coordinates that are used to derive the equations

of motion for the quarter car model are chosen such that the springs  $k_s$  and  $k_t$  are only relaxed when  $z_u=0$ ,  $z_s=0$ . In practice, however, the springs are never in their relaxed position due to the weight of masses  $m_s$  and  $m_u$ . In other words, due to gravity, the equilibrium point for  $(z_u, z_s)$ , i.e.  $(z_s eq1(t), z_u eq2(t))$ , never collocates with the location where the springs are relaxed (not loaded). In fact, the equilibrium points will be where a static balance between the weight of masses and the spring forced exists. The calculation of the equilibrium points  $z_s eq1(t)$  and  $z_u eq2(t)$  based on the masses  $m_s$  and  $m_u$ , spring constants  $k_s$ , and  $k_t$  and the gravity acceleration  $g$  is: After substituting the changes in equations of motion one will have

$$k_s z_{eq1}(t) - k_s z_{eq2}(t) + m_u g + z_{eq1}(t) k_t + m_u \left( \frac{d}{dt} 0 \right) = b_t \left( \frac{d}{dt} 0 \right) \quad (\text{III.3})$$

$$m_s g + k_s z_{eq2}(t) - k_s z_{eq1}(t) + m_s \left( \frac{d}{dt} 0 \right) = 0 \quad (\text{III.4})$$

The equilibrium points will be calculated as follows:

$$z_{eq1} = - \frac{(m_s + m_u)g}{k_t} \quad (\text{III.5})$$

$$z_{eq2} = - \frac{M_s g}{K_s} - \frac{(M_s + M_{us})g}{K_{us}} \quad (\text{III.6})$$

If the variable changes are written in the equations of motion, gravitational forces are subtracted from the equations of motion.

$$x_1(t) = z_u(t) + x_{eq1}, x_2(t) = z_s(t) + x_{eq2} \quad (III.7)$$

$$\frac{d}{dt} x_1(t) = \frac{d}{dt} z_u(t), \frac{d}{dt} x_2(t) = \frac{d}{dt} z_s(t) \quad (III.8)$$

$$\frac{d^2}{dt^2} x_1(t) = \frac{d^2}{dt^2} z_u(t), \frac{d^2}{dt^2} x_2(t) = \frac{d^2}{dt^2} z_s(t) \quad (III.9)$$

The equations of motion for using the new variables will be calculated as follows:

$$\begin{aligned} (z_u(t) - z_s(t))k_s + (z_u(t) - z_r(t))k_{us} + m_u \left( \frac{d^2}{dt^2} z_u(t) \right) = \\ -b_s \left( \frac{d}{dt} z_u(t) \right) - \left( \frac{d}{dt} z_{us}(t) \right) b_t - F_c + b_s \left( \frac{d}{dt} z_{us}(t) \right) + b_t \left( \frac{d}{dt} z_r(t) \right) \end{aligned} \quad (III.10)$$

$$(z_s(t) - z_u(t))k_s + m_s \left( \frac{d^2}{dt^2} z_s(t) \right) = b_s \left( \frac{d}{dt} z_u(t) \right) + F_c - b_s \left( \frac{d}{dt} z_s(t) \right) \quad (III.11)$$

We have the active suspension system dynamic where the effect of gravitational force is eliminated from the equations of motion. In other words, the relaxed position of the springs, i.e.  $z_u(t)=0$ ,  $z_s(t)=0$ , will be the equilibrium point of the system. Only inputs to this system are the control force and the road surface. The two transfer functions will be calculated as follows:

$$\frac{z_u}{z_r} = \frac{((Sb_t + k_t)(k_s + m_s S^2 + b_s S))}{\left( m_{us} S^4 m_s + (m_s b_t + m_u b_s) S^2 + (k_t m_s + k_s m_s + b_t b_s + m_u k_s) S^2 + (b_t k_s + k_t b_s) S + k_t k_s \right)} \quad (III.12)$$

$$\frac{z_s}{z_r} = \frac{(S^2 b_t b_s + (b_t k_s + k_t b_s)S + k_t k_s)}{m_u S^4 m_s + (m_s b_t + b_s m_s + m_u b_s)S^3 + (k_t m_s + k_s m_s + b_t b_s + m_u k_s)S^2 + (b_t k_s + k_t b_s)S + k_t k_s} \quad (\text{III.13})$$

### 3.2. State Space Representation

The Quanser Active Suspension System is modelled as a quarter vehicle model and allows the real system to be simulated. In order to simulate the real system and to test control strategies, the state space representation of the Quanser quarter vehicle model should be derived. State space matrices represent a set of linear differential equations that define the dynamics of the system. The two equations of motion in the quarter car model linear and time-invariant are shown as follows.

$$\frac{d}{dt}x(t) = Ax(t) + Bu(t) \quad (\text{III.14})$$

$$y(t) = Cx(t) + Du(t) \quad (\text{III.15})$$

The state-space approach is a convenient way to model the quarter-car model with multiple inputs and outputs. In this representation the states reflect the system performance parameters that have to be optimized. Moreover, this state space can be later used for observer and controller design. Due to the existence of four energy storage elements in quarter car model, the four state variables, inputs to the system, and the outputs can be defined as follows:

$$x = \begin{bmatrix} z_s(t) - z_u(t) \\ \frac{d}{dt} z_s(t) \\ z_u(t) - z_r(t) \\ \frac{d}{dt} z_u(t) \end{bmatrix}, \quad u = \begin{bmatrix} \frac{d}{dt} z_r(t) \\ F_c \end{bmatrix}, \quad y = \begin{bmatrix} z_s(t) - z_u(t) \\ \frac{d^2}{dt^2} z_s(t) \end{bmatrix} \quad (\text{III.16})$$

Where the first state represents suspension deflection. The second state is the vertical velocity of vehicle body. The third state is the tire deflection which is a measure of road handling. The fourth state is the velocity of tire. The first input to the system is the road surface velocity. The second input is the control action that will be later designed. The first measured output of the system is the suspension travel. Assuming that the vehicle body is equipped with an accelerometer, the second measured output of the system will be the body acceleration [16]. The matrices A, B, C, and D for the state space representation of the active suspension system will be as follows:

$$A = \begin{bmatrix} 0 & 1 & 0 & -1 \\ -\frac{k_s}{m_s} & -\frac{b_s}{m_s} & 0 & \frac{b_s}{m_s} \\ 0 & 0 & 0 & 1 \\ \frac{k_s}{m_u} & \frac{b_s}{m_u} & -\frac{k_t}{m_u} & -\frac{(b_s + b_t)}{m_u} \end{bmatrix} \quad (\text{III.17})$$

$$B = \begin{bmatrix} 0 & 0 \\ 0 & \frac{1}{m_s} \\ -1 & 0 \\ \frac{b_t}{m_u} & -\frac{1}{m_u} \end{bmatrix} \quad (\text{III.18})$$

$$C = \begin{bmatrix} 1 & 0 & 0 & 0 \\ -\frac{k_s}{m_s} & -\frac{b_s}{m_s} & 0 & \frac{b_s}{m_s} \end{bmatrix}, \quad D = \begin{bmatrix} 0 & 0 \\ 0 & \frac{1}{m_s} \end{bmatrix} \quad (\text{III.19})$$

### 3.3. System Transfer Functions

The state space representation that we derived in previous section is an example of a multi-input and multi-output system (MIMO) with two inputs, road surface velocity  $\frac{dz_r(t)}{dt}$  and controller force  $F_c$ , and two outputs, tire deflection  $z_u - z_r$  and acceleration of vehicle body  $\frac{d^2 z_s(t)}{dt^2}$  [17].

## IV. CONTROL DESIGN OF ACTIVE SUSPENSION SYSTEM

### 4.1. Introduction

The active suspension system includes a significant balance between the ride quality, rattle area and tire deflection. Advances in any of the three transfer functions in the passive suspension systems cause distortion in the other two transfer functions. In order to be able to design the control, two degree of freedom quarter vehicle models will be used in this section. The suspension system on each wheel will show the movement of the axis in one of the four wheels of the vehicle. The quarter vehicle model consists of an axle mass along with a quarter of the mass, springs  $k_s$  defining the stiffness of the suspension, a damper  $b_s$  which provides damping, and an active force actuator  $F_c$  which can be moved in both directions. The quarter car model is shown in Figure IV-1. The sprung mass  $m_s$  shows us a quarter of the vehicle body mass. The unsprung mass  $m_u$  is the equivalent mass from the axle and tire. The vertical stiffness of the tire is spring  $k_t$ . The variables  $z_s$ ,  $z_u$  and  $z_r$  shows us the vertical displacement from static equilibrium of the sprung mass, unsprung mass and the road. Differential equations of motion can be obtained by applying the second law of Newton to the model we consider to be the free-body diagram.

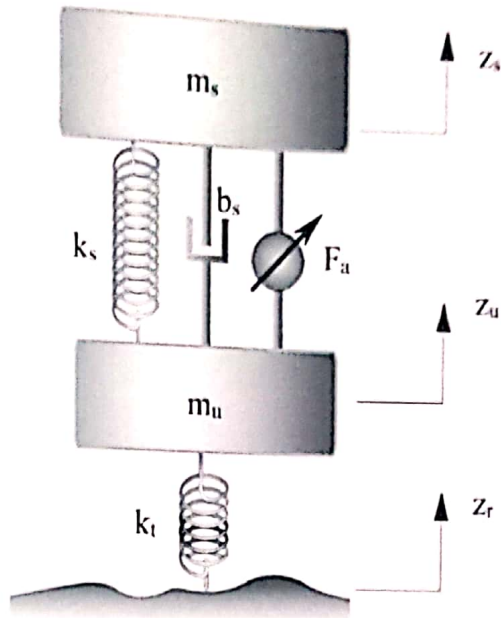


Figure IV-1. Active Quarter Car Suspension Model [17].

The equations of motion of the two-degree-of-freedom quarter-car suspension are:

$$m_s \ddot{z}_s + b_s(\dot{z}_s - \dot{z}_u) + k_s(z_s - z_u) = F_a \quad (\text{IV.1})$$

$$m_u \ddot{z}_u + k_t(z_u - z_r) + b_s(\dot{z}_s - \dot{z}_u) - k_s(z_s - z_u) = -F_a \quad (\text{IV.2})$$

The state space model of the quarter car active suspension system is:

$$\dot{x} = Ax + BF_a + L\dot{z}_r \quad (\text{IV.3})$$

where

$$x = [x_1 \ x_2 \ x_3 \ x_4]^T$$

$x_1 = z_s - z_u$  is deflection of suspension,

$x_2 = \dot{z}_s$  is the velocity of sprung mass,

$x_3 = z_u - z_r$  is deflection of tire,

$x_4 = \dot{z}_u$  is the velocity of unsprung mass.



$$A = \begin{bmatrix} 0 & 1 & 0 & -1 \\ -\frac{k_s}{m_s} & -\frac{b_s}{m_s} & 0 & \frac{b_s}{m_s} \\ 0 & 0 & 0 & 1 \\ \frac{k_s}{m_u} & \frac{b_s}{m_u} & -\frac{k_t}{m_u} & -\frac{(b_s + b_t)}{m_u} \end{bmatrix} \quad (IV.4)$$

$$B = \begin{pmatrix} 0 \\ 1/m_s \\ 0 \\ 1/m_u \end{pmatrix} \quad (IV.5)$$

$$C = \begin{bmatrix} 1 & 0 & 0 & 0 \\ -\frac{k_s}{m_s} & \frac{b_s}{m_s} & 0 & \frac{b_s}{m_s} \end{bmatrix} \quad (IV.6)$$

$$D = \begin{bmatrix} 0 & 0 \\ 0 & 1/m_s \end{bmatrix} \quad (IV.7)$$

$$L = \begin{pmatrix} 0 \\ 0 \\ -1 \\ 0 \end{pmatrix} \quad (IV.6)$$

There are two different methods to control active suspension system. The first one is feedforward method and the second is feedback method. In the feedforward method, controller measures the input signal and calculates control signal according to input disturbance to cancel the disturbance. In other words, the controlled variable is a precautionary procedure without further deterioration. On the other hand, in feedback control method, the controller measures the system response of input disturbance and calculates control signal according to response of system to cancel the disturbance. In

theory, a feedforward control method can provide better performance than feedback method. But to implement the feedback method to a system is easier than feedforward method. The transfer functions to be used in this study are given below: [17]

The transfer function of vehicle body acceleration is:

$$H_A(s) = \frac{\ddot{z}_x(s)}{\ddot{z}_r(s)} \quad (IV.11)$$

Rattle space transfer function is:

$$H_{RS}(s) = \frac{z_x(s) - z_u(s)}{\dot{z}_r(s)} \quad (IV.12)$$

Tire deflection transfer function is:

$$H_{TD}(s) = \frac{z_u(s) - z_r(s)}{\dot{z}_r(s)} \quad (IV.13)$$

The purpose of the active suspension system is to minimize the transfer functions with the selected controller. Therefore, the state vector matrix is selected to minimize these values. States feedback is very important in the control of the active suspension. All situations must be appropriate when designing the control. It should also be possible to measure these conditions. These situations can be measured with the help of sensors in the active suspension system. But it is very difficult to measure these situations in the real vehicle. In this study, I will explain my observations using a linear quadratic regulator. In the Figure IV-2, is shown The Simulink model of the active suspension system for quarter car model which built by using the above equations IV-1 and IV-2.

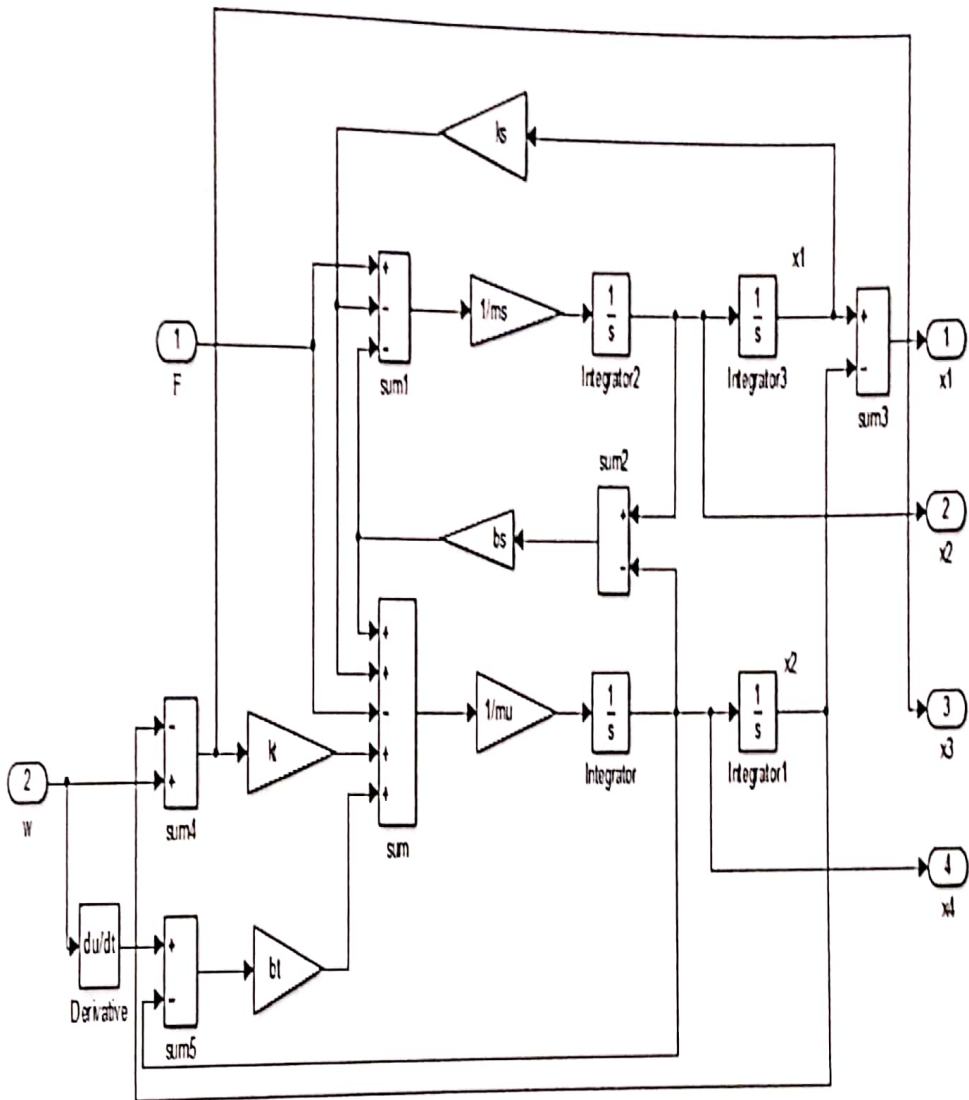


Figure IV-2. Simulink diagram of active suspension system

## V. CONTROL METHODS

Linear or non-linear control methods are used for the control of active suspension systems. There is an actuator that can be controlled with feedback between the vehicle body and the wheels. The linear control method has a low performance compared to non-linear control method. For a better driving safety and comfort, a non-linear controller should be designed. Examples of linear active suspension control methods are PID control Skyhook control, Groundhook Control,  $H^\infty$  control and LQR method. Even if the controls applied with these methods reach the performance target, they can only be performed within a limited frequency range.

### 5.1. Controllability and Observability

Before applying a control method, we have to check the states. If there are no controllable and observable state, system will be controllable and observable. The code for checking controllability and observability is given in Appendix A. And the system is controllable and observable.

### 5.2. Implementing of Control Methods

In this part of the study, the effect of the LQR, skyhook and groundhook active suspension system, which is formulated in the Quanser Active Suspension test device, on the performance criteria will be examined. The system's transition matrix  $A$  has dimensions of 4-by-4, there should be four open-loop poles. Also we can say there are 4 storage element 2 springs and 2 dampers. There are 2 different resonant frequencies because there are two different spring and damper. One of them is suspension system and the other one is tire.

Resonant frequency formula is:

$$w_{resonance} = \sqrt{\frac{K}{m}} \quad (V-1)$$

So  $w_{resonant}$  of the tire is 50 and  $w_{resonant}$  of the suspension system is 19.16.

The Simulink block diagram used in the experiments and simulations is as in Figure IV.1. It includes experiment part and simulation part. So we can measure both actual and simulation results together.

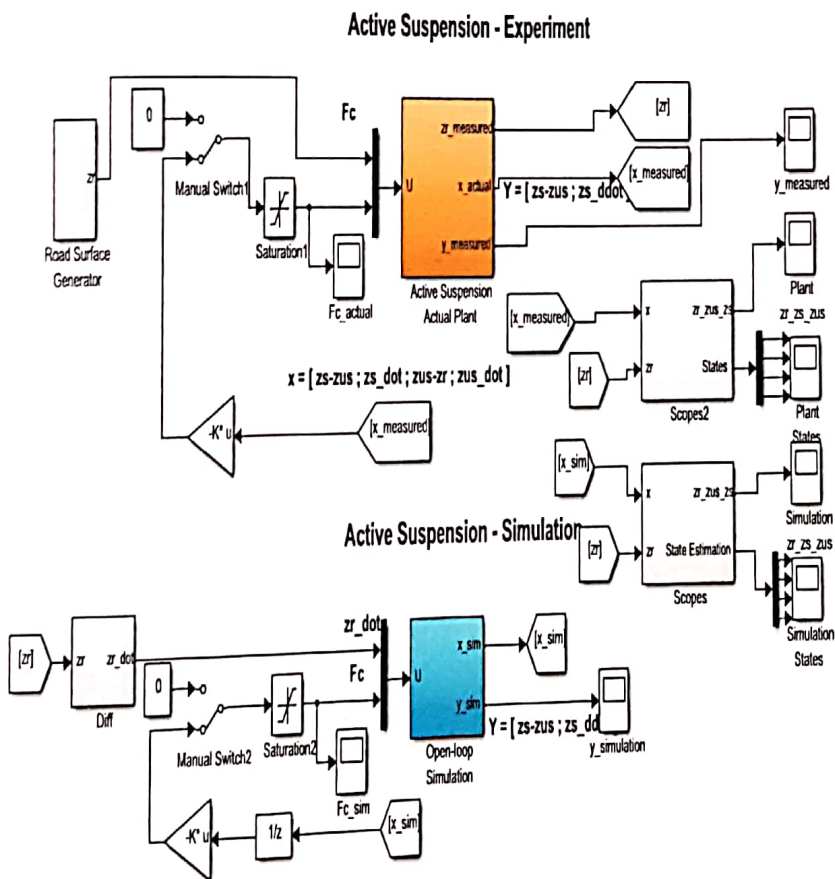


Figure V-1. Active Suspension Plant Simulink Blocks

Also this SIMULINK system has Road Surface Generator (Figure V-2), Road simulator (Figure V-3), Vehicle Body (Figure V-4), Suspension (Figure V-5), Control Actuator (Figure V-6).

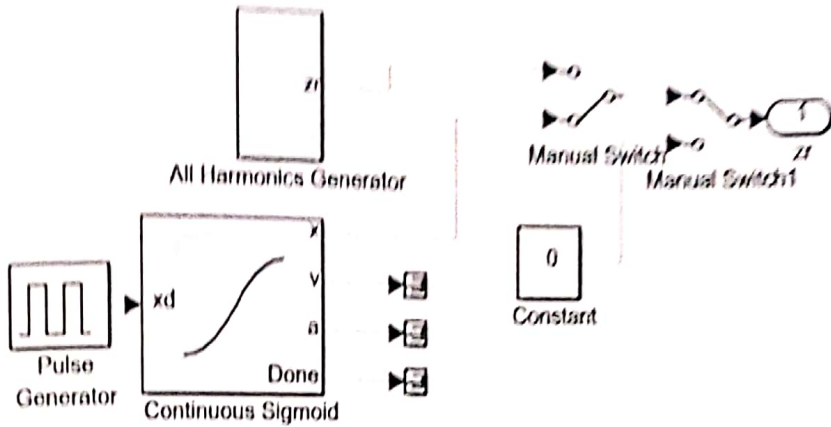


Figure V-2. Road Surface Generator Block

The road surface generator block sends the road signal which we desired to Quanser Active Suspension System's road profile servo motor. There are two type road profile signal in the road surface generator block. One of them is random signal which has changing frequency and the other one is square wave signal.

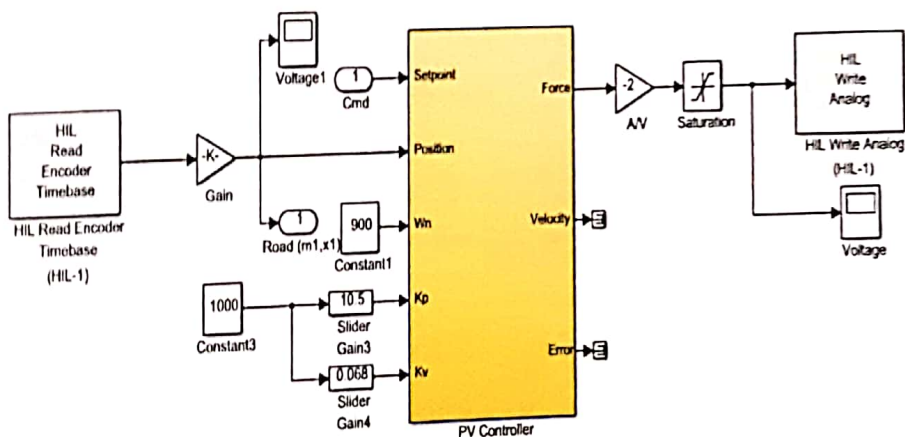


Figure V-3. Road Simulator Block

To have good performance in the Hardware in the Loop simulation, input must be in our control. It is not enough to give the road signal to the motor. Also we must apply a control algorithm to get close road signal that we give.

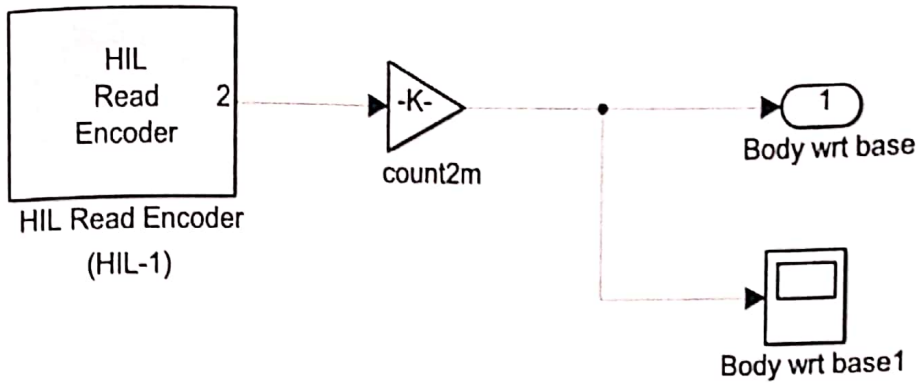


Figure V-4. Vehicle Body Block

In this block we get data from the encoder that measures the distance body to base. Also we multiply with a constant to change the unit.

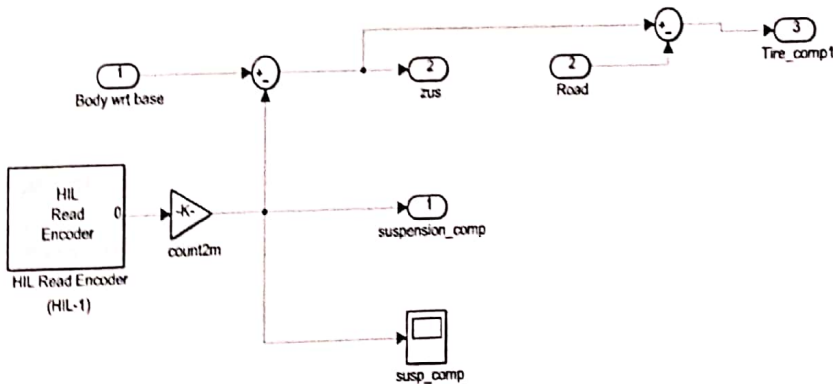


Figure V-5. Suspension Block

In this block, we get data from the other encoder and calculate suspension compression and tire compression.

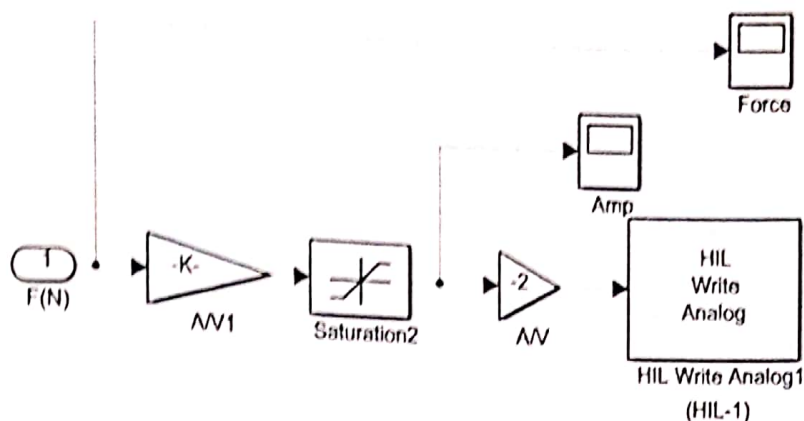


Figure V-6. Control Actuator Block

In this block we send the control signal to control actuator. And control actuator applies force to the system according to control signal. Again there is a gain because we want to apply -5 to +5 voltage to the system and after gain there is a saturation block. It protects the motor and the AMPAQ from high voltage that control algorithm generates.

### 5.3. Linear Quadratic Regulator (LQR) Control

In the active suspension system, it is necessary to minimize the vertical body acceleration, suspension deflection amount and wheel deviation amount expected from the controller. Equations V-1 and V-2 are general space state formulations. Where  $d$  is the system of noise input,  $u$  control input and the variables  $z$  consist of the sprung mass acceleration, the suspension deflection and the tire deflection.

$$\dot{x} = Ax + B_1d + B_2u \quad A \in R^{n \times n}, B_1 \in R^n, B_2 \in R^n \quad (V-2)$$

$$Z = C_1x + D_{12}u \quad C_1 \in R^{m \times n}, D_{12} \in R^{m \times 1} \quad (V-3)$$



The above-state space formulation makes the control problem  $u$  for noise input, minimizing  $z$  variables. This type of control problems in the literature  $H_2$  is called the optimal control problem [18]. The optimization procedure for an LQR controller consists of determining the control input  $F_c$  which minimizes the following performance index:

$$J = \int_0^{\infty} z^T z dt = \int_0^{\infty} [x^T C_1^T C_1 x + 2x^T C_1^T D_{12} u + u^T D_{12}^T D_{12} u] dt \quad (V-4)$$

The solution of the LQR problem is given in the solution of the given equation (V-5).

$$\begin{aligned} u &= -(D_{12}^T D_{12})^{-1} B_2^T P x - (D_{12}^T D_{12})^{-1} (C_1^T D_{12})^T x \\ &= -(D_{12}^T D_{12})^{-1} [B_2^T P + (C_1^T D_{12})^T] x \end{aligned} \quad (V-5)$$

If the suspension system performance criteria are written to the LQR problem formulation given by equation (V-3), the equation takes the form indicated by equation (V-5). The new variables  $\rho_1, \rho_2, \rho_3$  and  $\rho_4$  can be defined as the weighting coefficients. According to these coefficients, the order of importance can be listed among the performance values.

$$J = \left[ \int_0^{\infty} \ddot{z}_s^2 + \rho_1 (z_s + z_u)^2 + \rho_2 \dot{z}_s^2 + \rho_3 (z_u - z_r)^2 + \rho_4 \dot{z}_u^2 dt \right] \quad (V-6)$$

If this optimization equation is written in the solution given with the equation (V-3).

$$\begin{aligned} \ddot{z}_s^2 &= \frac{1}{m_s^2} [k_s^2 x_1^2 + b_s^2 x_2^2 + b_s^2 x_4^2 + F_a^2 + 2k_s b_s x_1 x_2 - 2k_s b_s x_1 x_4 - 2b_s^2 x_2 x_4 \\ &\quad - 2k_s x_1 F_a - 2b_s x_2 F_a + 2b_s x_4 F_a] \end{aligned} \quad (V-7)$$

Thus, the equation (V-7) is ensured.

$$\ddot{z}_s^2 + \rho_1(z_s - z_u)^2 + \rho_2\dot{z}_s^2 + \rho_3(z_u - z_r)^2 + \rho_4\dot{z}_u^2 = x^T Qx + 2x^T N F_a + F_a^T R F_a \quad (V-8)$$

The containing system parameters Q, N matrix and R, value used in equation (V-8), are given in equation (V-9).

$$Q = \begin{bmatrix} \frac{k_s^2}{m_s^2} + \rho_1 & \frac{b_s k_s}{m_s^2} & 0 & -\frac{b_s k_s}{m_s^2} \\ \frac{b_s k_s}{m_s^2} & \frac{b_s^2}{m_s^2} + \rho_2 & 0 & -\frac{b_s^2}{m_s^2} \\ 0 & 0 & \rho_3 & 0 \\ -\frac{b_s k_s}{m_s^2} & -\frac{b_s^2}{m_s^2} & 0 & \frac{b_s^2}{m_s^2} + \rho_4 \end{bmatrix}, N = \begin{Bmatrix} -\frac{k_s^2}{m_s^2} \\ -\frac{b_s^2}{m_s^2} \\ 0 \\ \frac{b_s^2}{m_s^2} \end{Bmatrix} \text{ and } R = \frac{1}{m_s^2} \quad (V-9)$$

According to the output given with the equation (V-7), the performance index can be written again (V-9).

$$J = \left[ \int_0^\infty (x^T Qx + 2x^T Nu + u^T Ru) dt \right] \quad (V-10)$$

If the optimum control performance problem given by the solution method in the equation (V-4) is applied to equation (V-9)  $F_a = -kx$  state feedback solution will be generated under the noise input by d and minimizing the values indicated by z. The matrix given by K (V-11) can be defined as feedback matrix which is the solution set of the Ricatti equation (V-10). This solution set is given in (V-11) equation.

$$(A - BR^{-1}N)^T P + P(A - BR^{-1}N) + (Q - N^T R^{-1}N) - PBR^{-1}B^T P = 0 \quad (V-11)$$

$$K = R^{-1}(B^T P + N) \quad (V-12)$$

As seen in the equation given by (V-11), the K gain matrix consists of two parts,  $R^{-1}B^T P$  and  $R^{-1} N$ .  $R^{-1} N$  consists of fixed parameters of the system and has no connection with the solution of the Ricatti equation or the weighting coefficients used in the performance index.

The result of this is that the K gain matrix depends on the weighting coefficients  $\rho_1, \rho_2, \rho_3$  and  $\rho_4$  used in the first part performance index expressed by  $R^{-1}B^T P$  and the second part, expressed as  $R^{-1} N$ , is the duty of eliminating the passive forces caused by the passive spring and damper and expressed by  $k_s x_1 + b_s(x_2 - x_4)$ .

Thus, it is concluded that the total force acting on the LQR controlled active suspension system is independent of the passive elements of the system expressed in k and b. Even if the values of these passive elements change, the control will be eliminated by the second part of the law  $R^{-1} N$  [19].

### 5.3.1. Performance Studies of LQR Control Method

The effect of the controller on the performance criteria is directly related to the weighting coefficients used in the performance index. Therefore, different weighting coefficients were used for the experiments. Adjustments were made according to the desired performances. Table V-1. shows the weighting coefficients used in the experiments with LQR. In these parameters, the acceleration of the vehicle body and the amount of deflection of tire were analysed.

Table V-1. Weighting coefficients in LQR design.

	$\rho_1$	$\rho_2$	$\rho_3$	$\rho_4$	$R$
test <sub>1</sub>	0.01	0.01	0.01	0.01	0.001
test <sub>2</sub>	100	10000	1	100	0.001
test <sub>3</sub>	100	1	10000	100	0.001
test <sub>4</sub>	200	100	200	100	0.001

According to the first weighting coefficients, the acceleration of the vehicle in the vertical direction and amount of tire deflection are compared with the passive suspension system. As can be observed from the Figure V-7. And V-8.

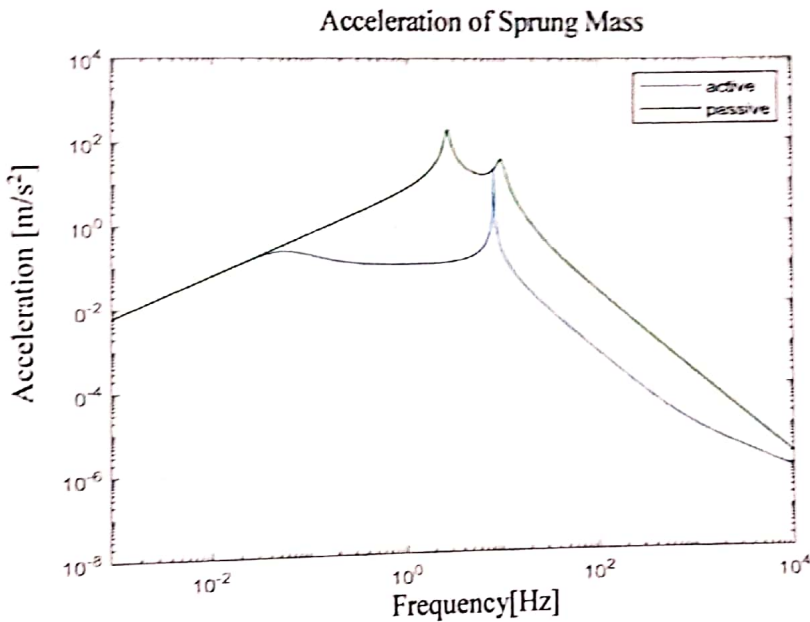


Figure V-7. Vertical acceleration of vehicle body

The active suspension system has a better response in terms of vertical acceleration performance at all frequencies than passive suspension.

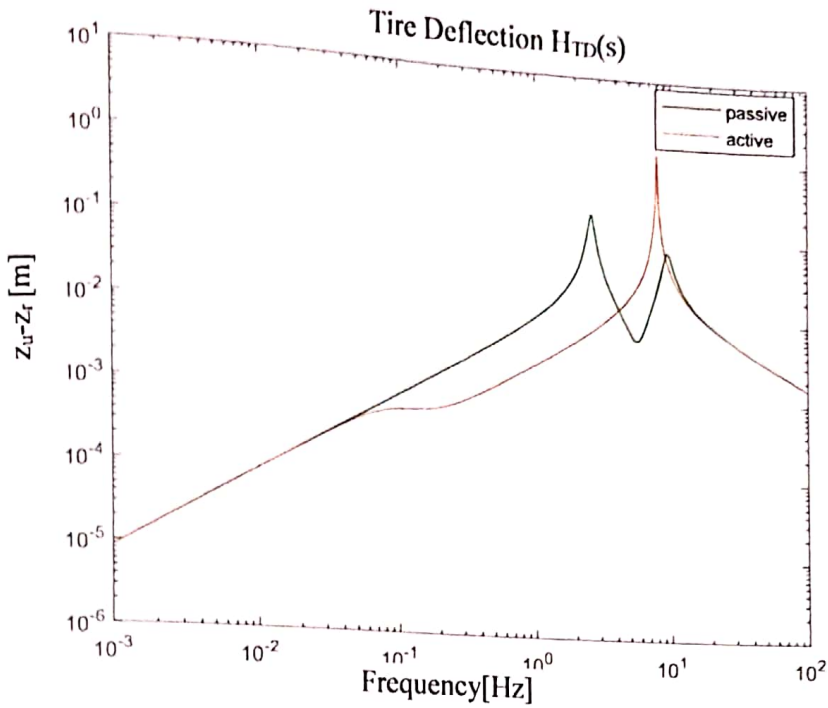


Figure V-8. Tire Deflection

The effect of active suspension on tire deflection is given in Figure V-8. When the results are evaluated, it shows that the tire deflection of the active suspension system decreases in low frequency values. However, in frequency values between 3 Hz and 9 Hz, there was a worse deflection than the passive suspension.

If the acceleration weighting coefficient is increased and the tire deflection coefficient is reduced in the second weighting coefficients, the results will be shown with Figure V-9. and V-10.

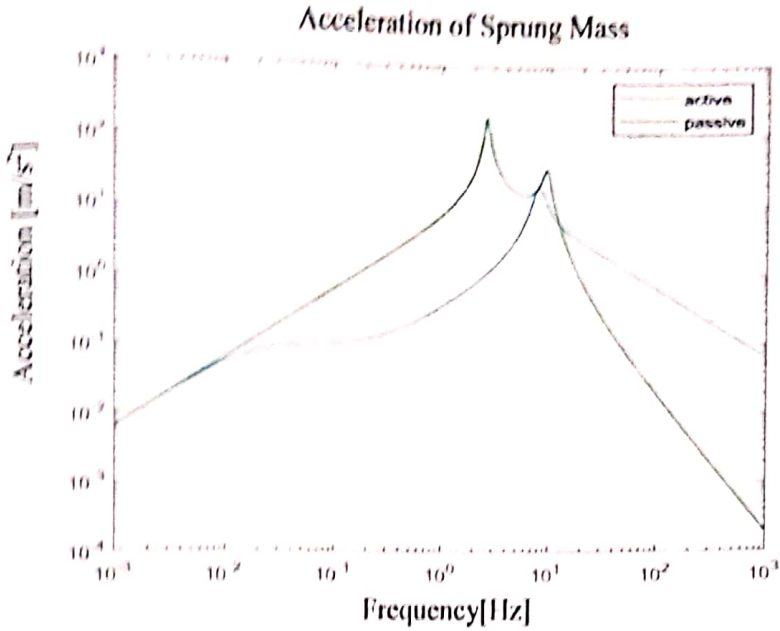


Figure V-9. Vertical acceleration of vehicle body

In the new weighting coefficients, the acceleration performance of the active suspension in the vertical direction is better than the passive suspension at frequencies up to 15 Hz.

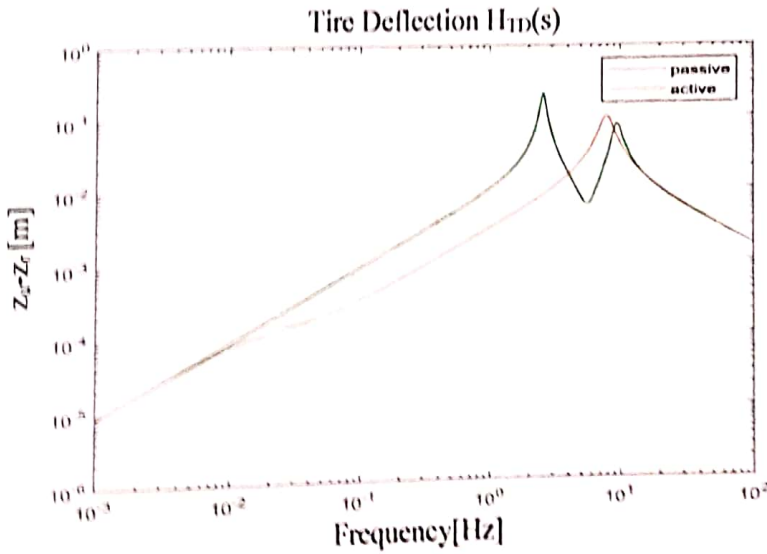


Figure V-10. Tire Deflection

The amount of tire deflection of active suspension is better than passive suspension at frequencies up to 3 Hz and higher than 12 Hz.

According to the third weighting coefficients, If the acceleration weighting coefficient is reduced and the tire deflection coefficient is increased, the results will be shown with Figure V-11. and V-12.

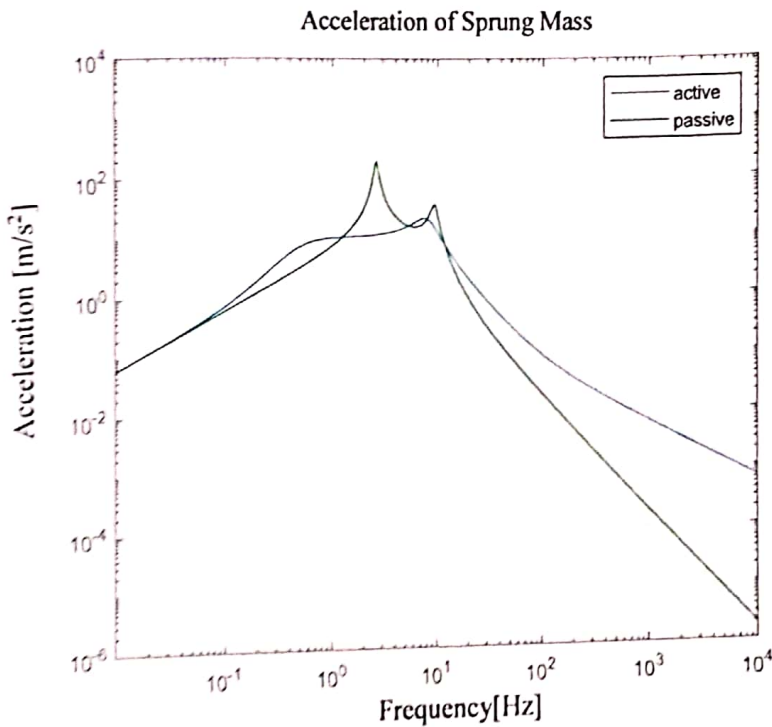


Figure V-11. Vertical acceleration of vehicle body

According to the new weightings, the acceleration performance of the active suspension in the vertical direction is shown in Figure V-11. Since the acceleration performance weighting coefficient decrease it gave a worse result than passive suspension at frequencies higher than 1 Hz.

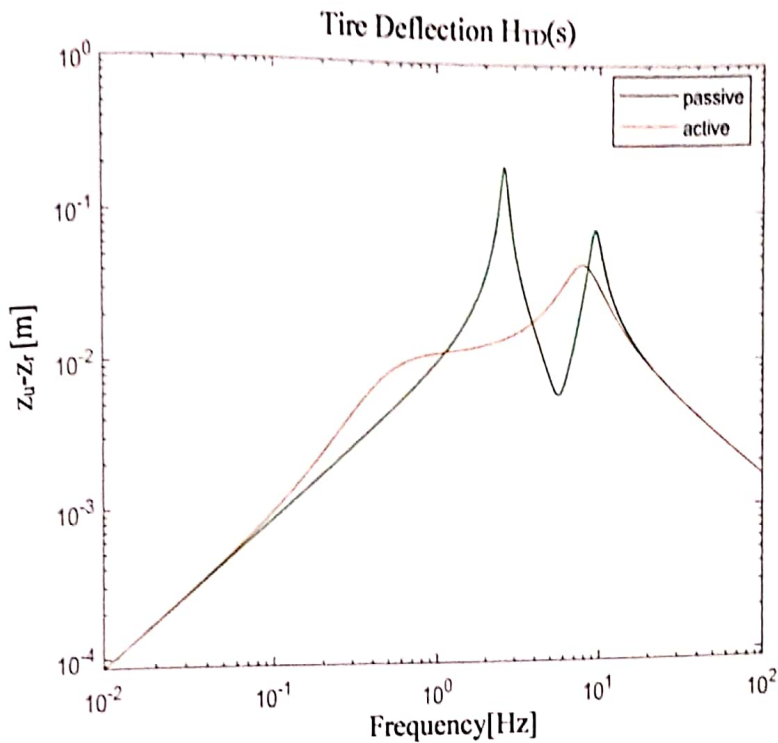


Figure V-12. Tire Deflection

The effect of the new controller on the tire deflection is given in Figure V-12. According to the result obtained, it was observed a noticeable decrease in the tire deflection amount performance of the system in the low frequency range up to 1 Hz. However, it can be said that in the frequency range between 1-3 Hz and 8-20 Hz, the performance better than the passive system.

The last weighting coefficients, the acceleration of the vehicle in the vertical direction and the tire deflection are compared with the passive suspension system. If the acceleration coefficient and the tire deflection coefficient increase equal as can be observed from the Figure V-13. and V-14.



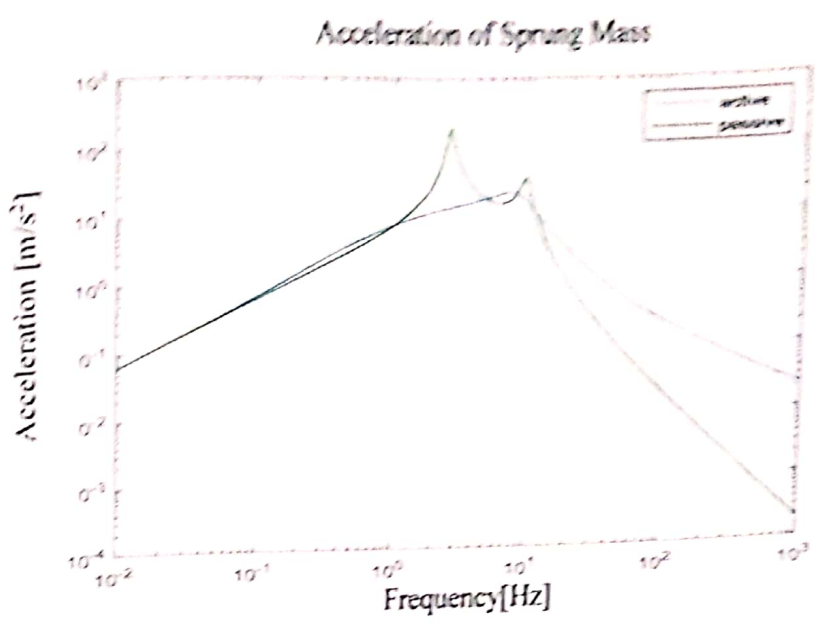


Figure V-13. Vertical acceleration of vehicle body

According to the equal weightings coefficient, the acceleration performance of the active suspension in the vertical direction is shown in Figure V-13. The acceleration performance worse result than passive suspension at frequencies up to 1 Hz and higher than 12 Hz.

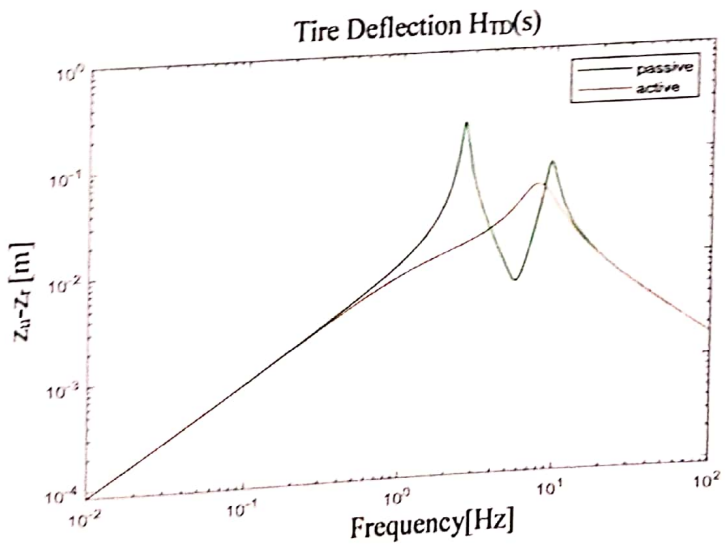


Figure V-14. Tire Deflection

In equal weighting coefficients, the tire deflection amount of *active suspension* system has a better result up to 3 Hz and in the frequencies range 9-20 Hz than *passive suspension*.

According to the selected parameters, it was observed that it was not possible to provide all four performances continuously at certain frequencies.

The results of the simulation and experiment studies with the different inputs are detailed in the next part of study.

#### 5.4. Skyhook control

In the Skyhook control, it is aimed to try to damp the movement of the vehicle body with the help of a virtual damper. A damper, which is considered to be tied to the sky, has a much better damping than the tire. The Sky-Hook control is used in both semi active and active suspension systems. Since it cannot provide two-way force in the semi active suspension system, the optimum performance contribution from the virtual damper is only possible with the active suspension system. The Skyhook control method is system feedback as in the LQR control method. Unlike the LQR method, only the body speed is feedback and multiplied by a gain factor. The force to be applied to the system occurs this way. Only the speed of the vehicle can be checked and the driving quality can be improved, but the performance of other situations in the system is reduced. The Skyhook Force is calculated as in equation (V-11) [8].

$$F_{sky} = -C_{sky} \dot{z}_s \tag{V-11}$$

The scheme of the Skyhook control system is as shown in Figure V-15.

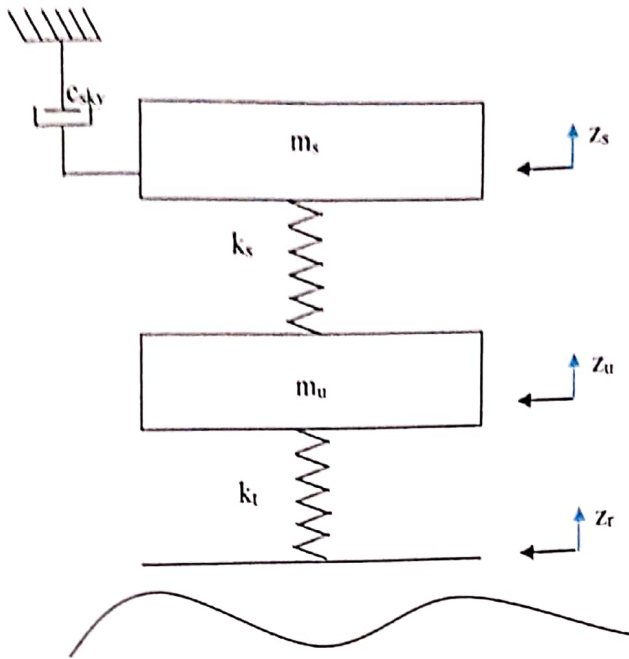


Figure V-15. Structure of skyhook control

#### 5.4.1. Performance Studies of Skyhook Control Method

Three different  $c_{sky}$  values were used to see the effect of the Skyhook controller on vehicle body acceleration and tire deflection. The coefficients are given in the table V-2. below.

Table V-2. Coefficients in Skyhook design

$C_{sky}$	$C_{sky}$	$C_{sky}$
1000	10000	100000

The results with the  $c_{sky}$  values given in table V-2. are shown in Figures from V-16. to V-21.

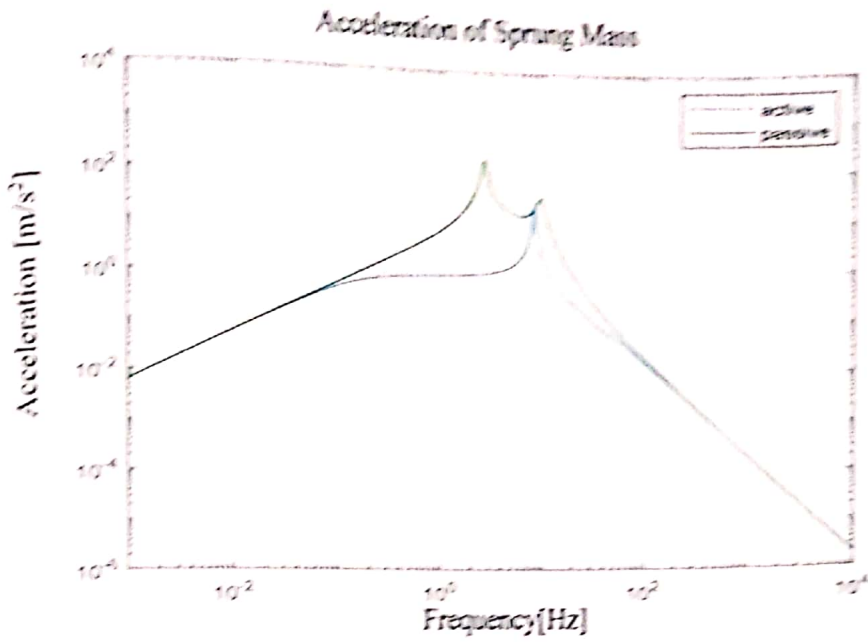


Figure V-16. Sprung mass acceleration for  $c_{sky}=1000$

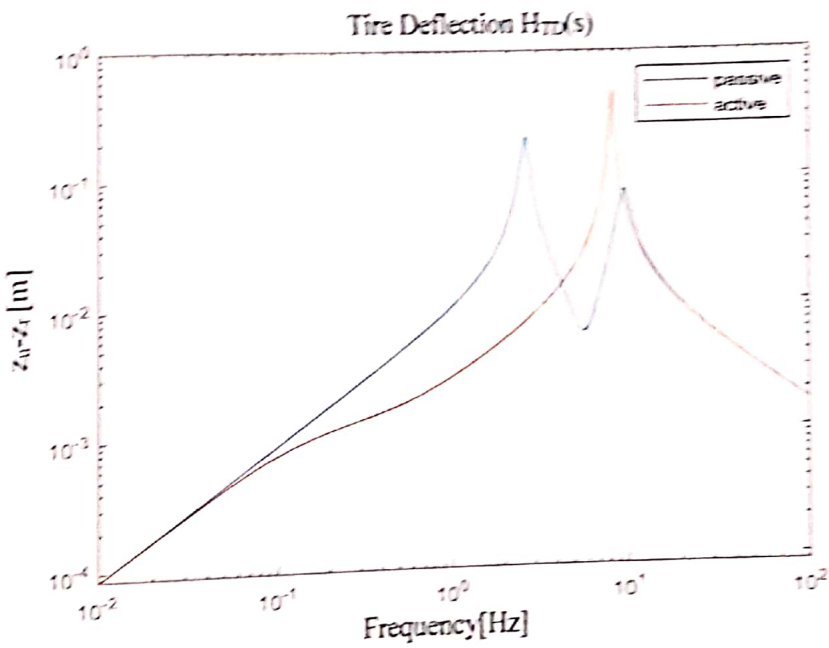


Figure V-17. Tire deflection for  $c_{sky}=1000$

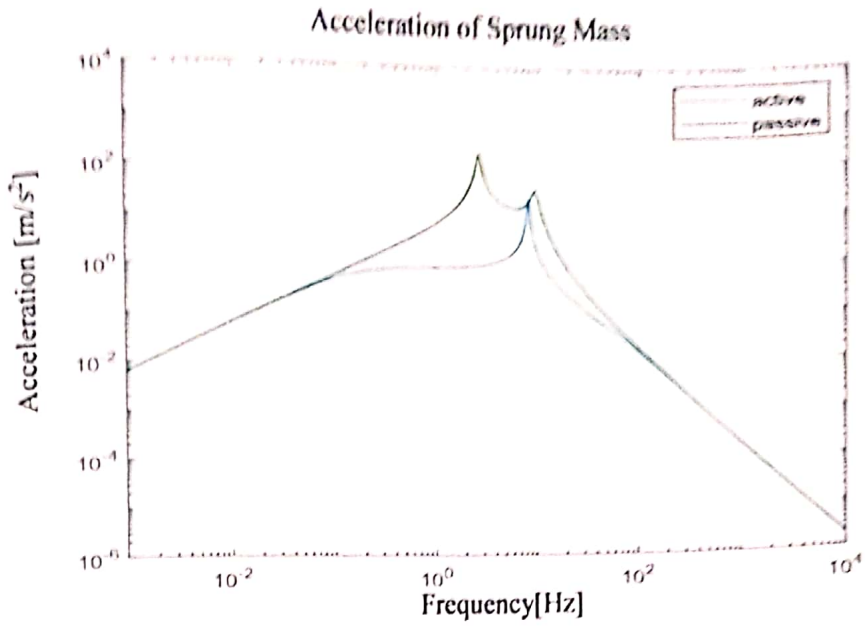


Figure V-16. Sprung mass acceleration for  $c_{sky}=1000$

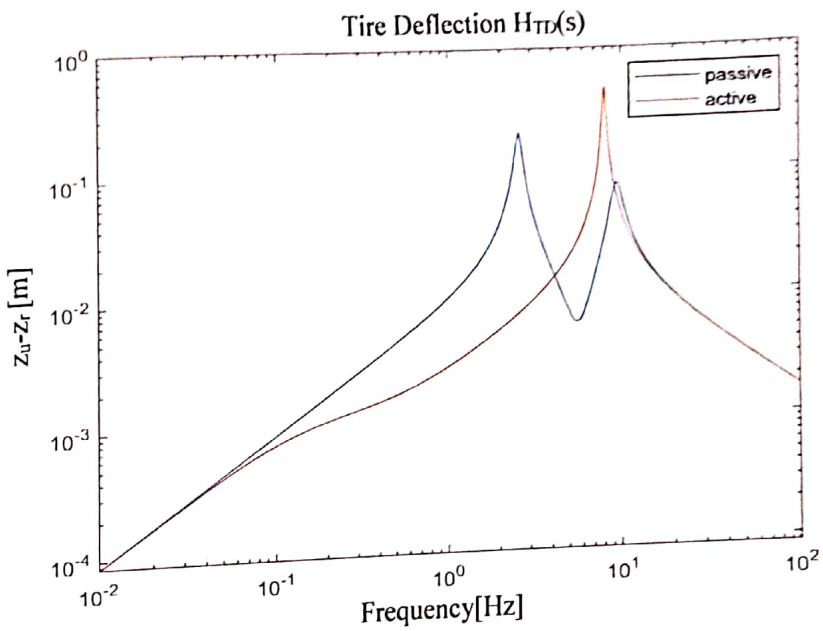


Figure V-17. Tire deflection for  $c_{sky}=1000$

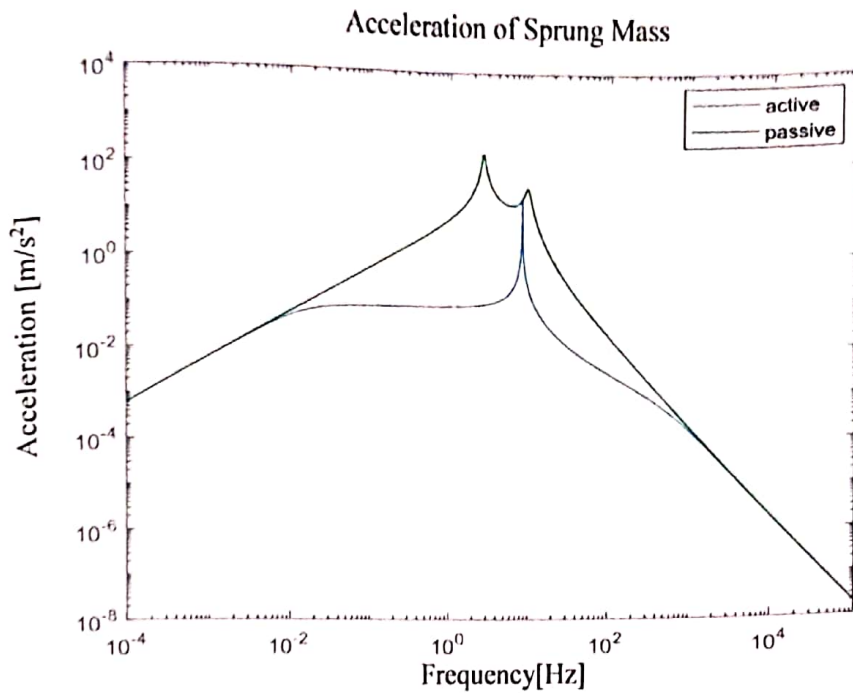


Figure V-18. Sprung mass acceleration for  $c_{sky}=10000$

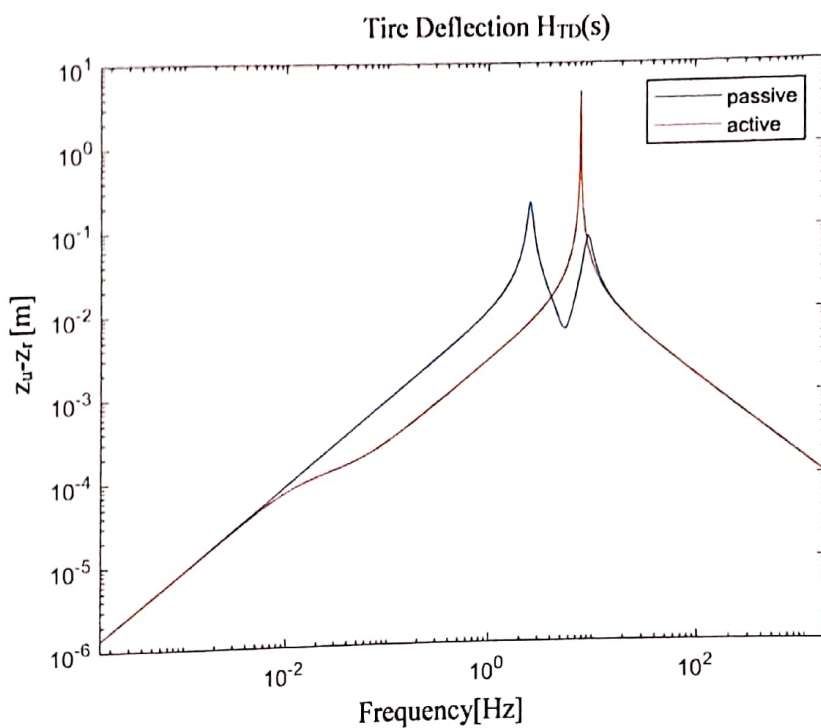


Figure V-19. Tire deflection for  $c_{sky}=10000$

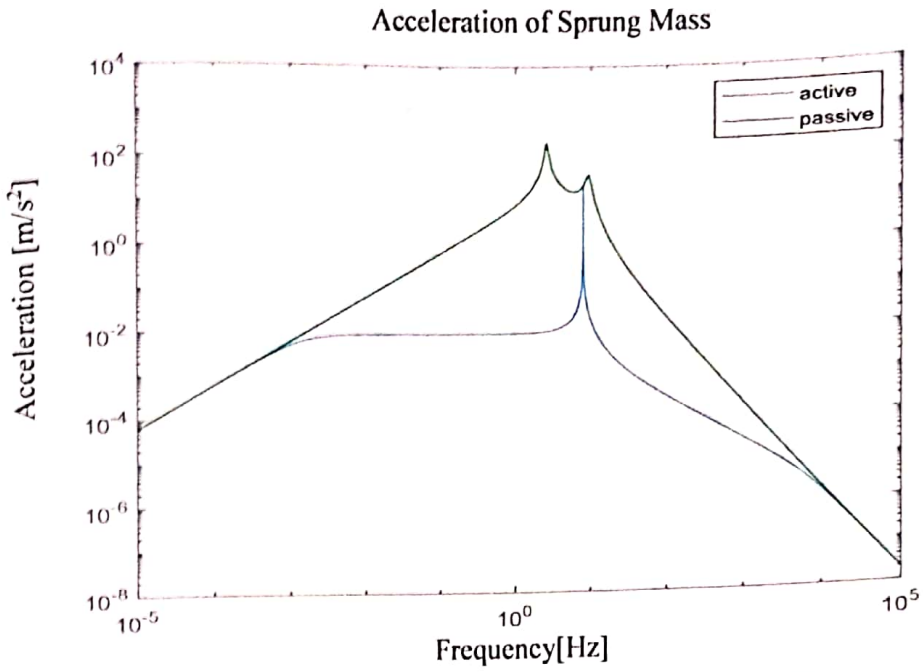


Figure V-20. Sprung mass acceleration for  $c_{sky} = 100000$

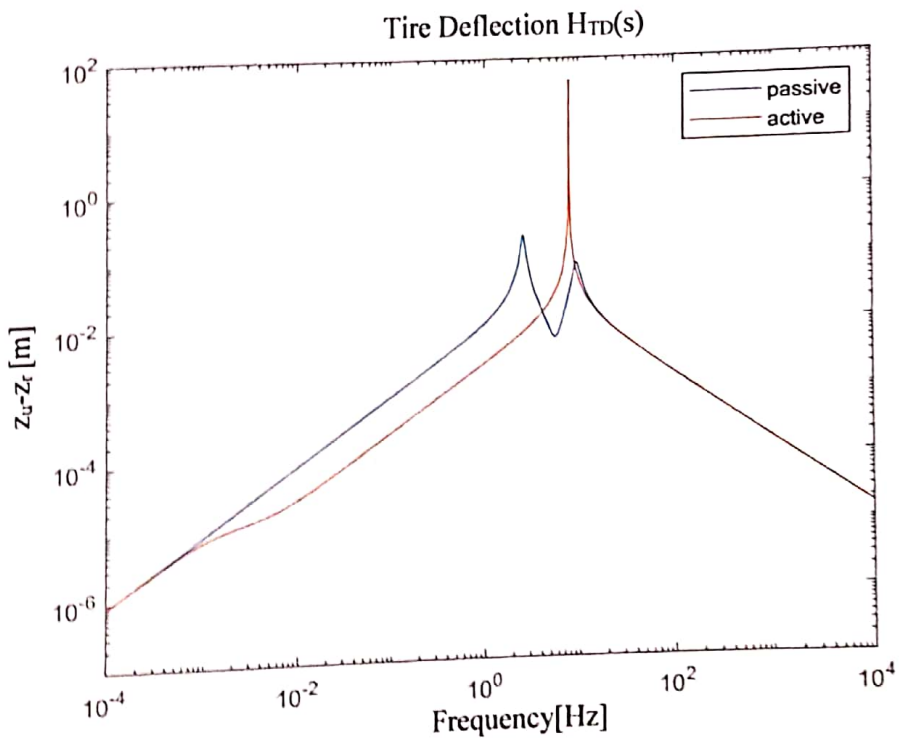


Figure V-21. Tire deflection for  $c_{sky} = 100000$

The Skyhook controller of the active suspension shows very satisfactory results. As the amount of gain is increased, the vertical acceleration decreases at all frequencies, it can be said a more comfortable ride. The effect of active suspension on tire deflection is good result in low frequency values. However, there is a worse deflection than the passive suspension in higher frequency values.

### 5.5. Groundhook control

The Groundhook control method is like the Skyhook control method. It is designed with the help of a virtual fixed damper to reduce vibrations in the load of the wheel. The velocity on the vertical axis of the tire is designed as a control input. The Groundhook control method is system feedback as in the LQR control and skyhook control methods. The Groundhook Force is calculated as in equation (V-12) [9].

$$F_{gnd} = c_{gnd} \dot{z}_r \quad (V-12)$$

The scheme of the Groundhook control system is as shown in Figure V-22.

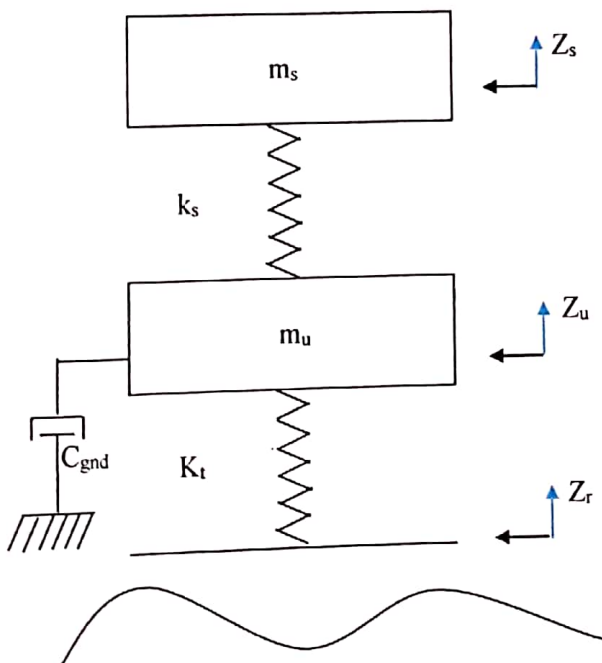


Figure V-22. Structure of Groundhook control



### 5.5.1. Performance Studies of Groundhook Control Method

Three different  $c_{gnd}$  values were used to see the effect of the groundhook controller on vehicle body acceleration and tire deflection. The coefficients are given in the table V-3. below.

Table V-3. Coefficients in Groundhook design

$C_{gnd}$	$C_{gnd}$	$C_{gnd}$
100	1000	10000

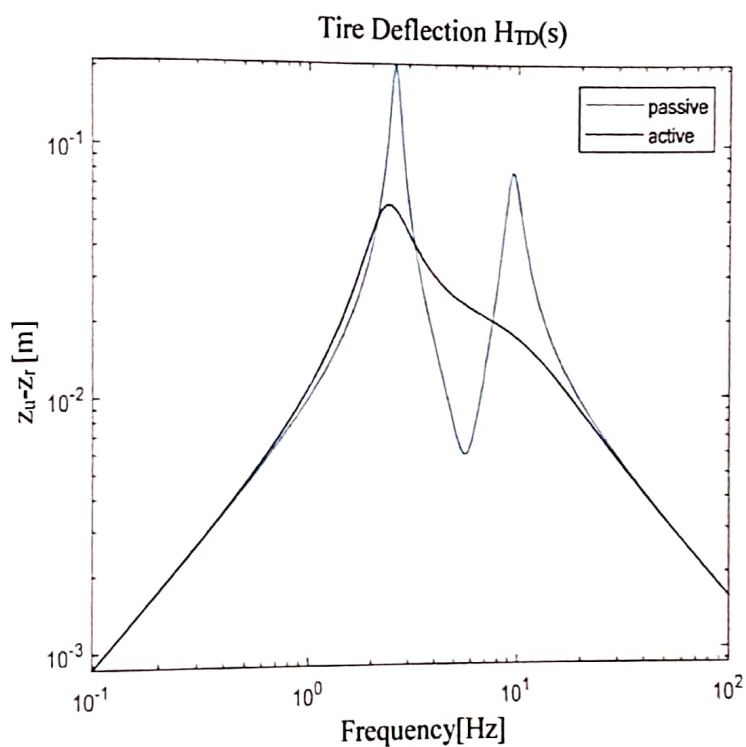


Figure V-23. Tire deflection for  $c_{gnd}=100$

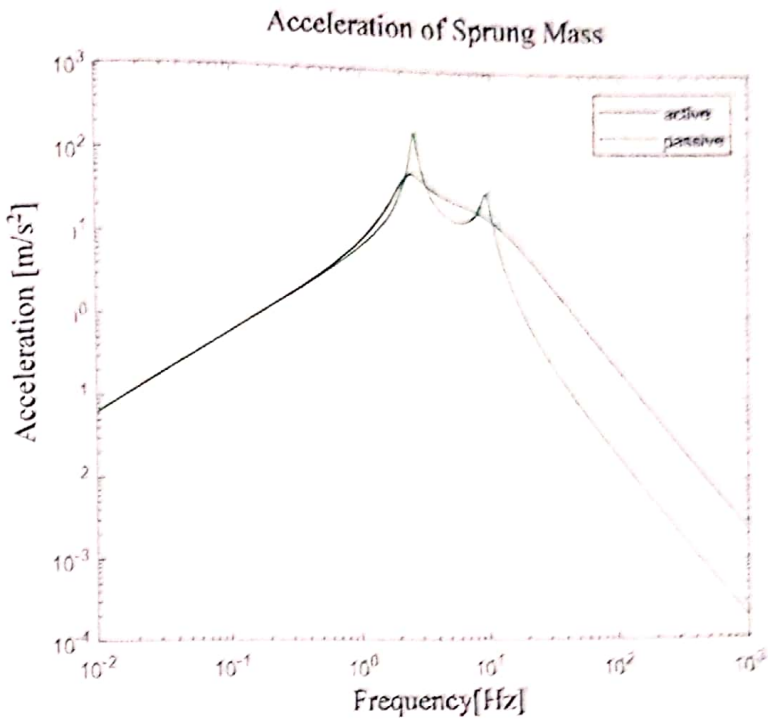


Figure V-24. Sprung mass acceleration for  $c_{\text{spr}}=100$

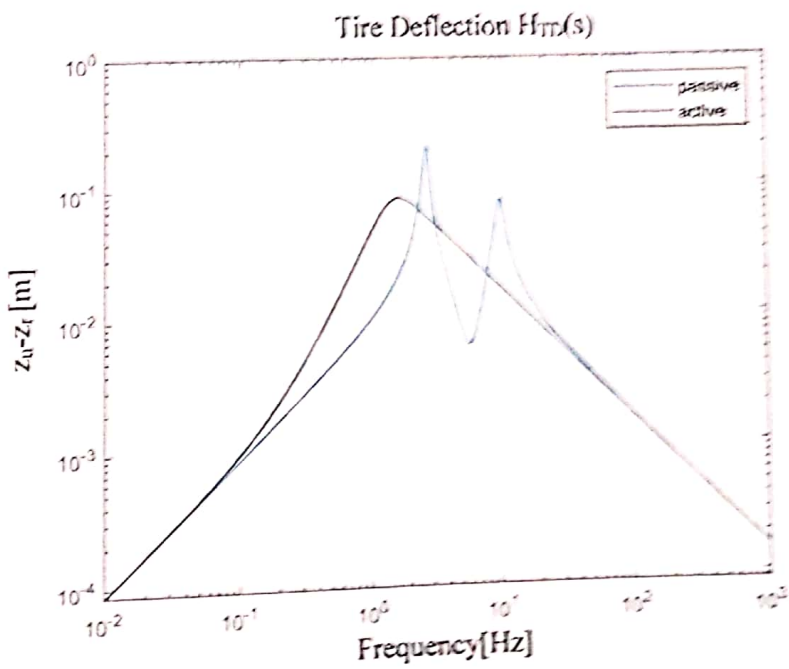
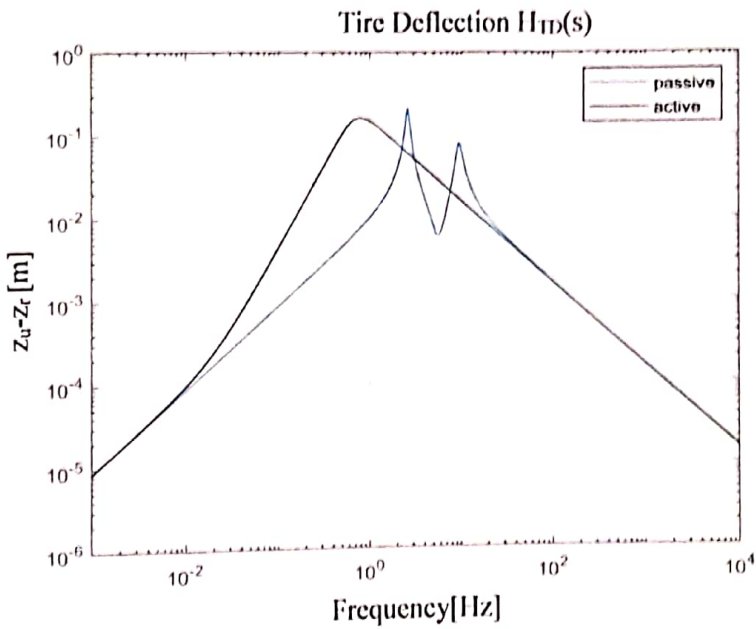
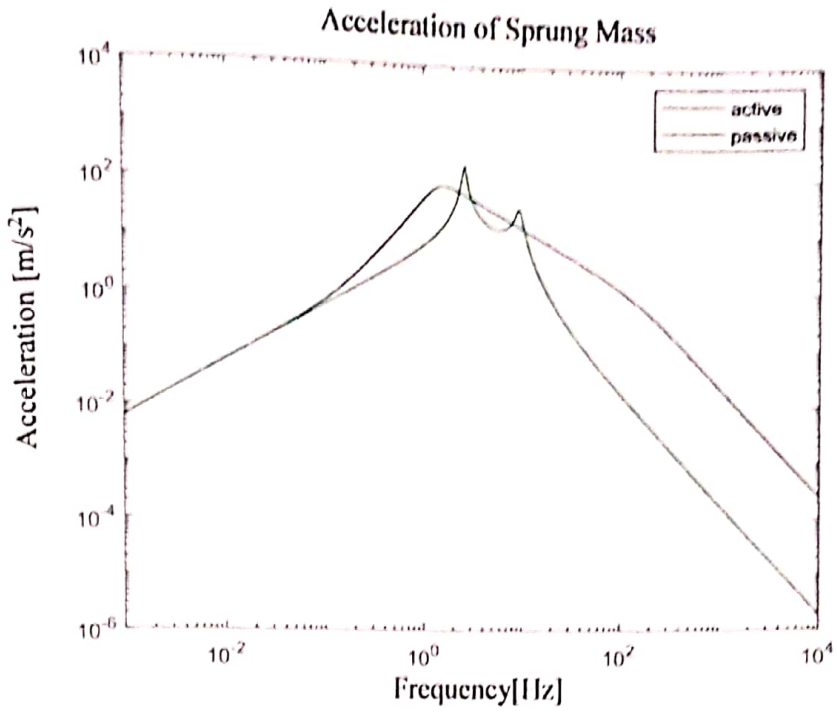


Figure V-25. Tire deflection for  $c_{\text{spr}}=1000$



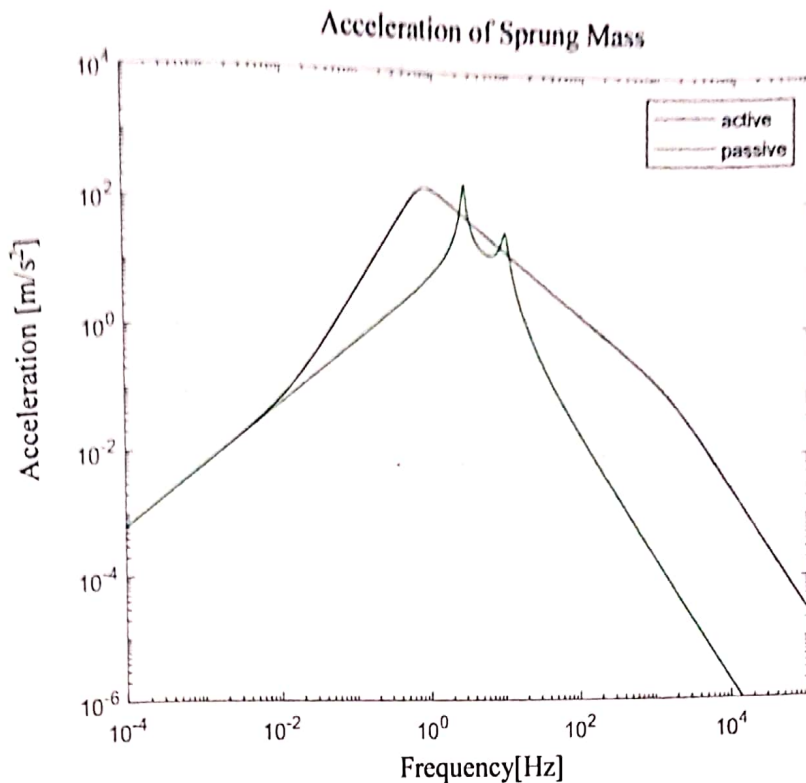


Figure V-28. Sprung mass acceleration for  $c_{\text{gnd}}=10000$

According to the results, the acceleration of the vehicle in the vertical direction and amount of tire deflection are compared with the passive suspension system. It was observed that there were improvements on the tire deflection. But the acceleration of the sprung mass of the active suspension was worse than the passive suspension. As the amount of gain is increased, vehicle body acceleration has increased. The Groundhook controller improves the amount of tire deflection and cannot improve vehicle body acceleration.

## VI. IMPLEMENTATION AND EXPERIMENTAL RESULTS

The responses of the active suspension system with different controllers which were designed with different weighting coefficients given in Table V-1. were observed.

The obtained results with LQR controller when an input of a square wave signal and a random signal are applied to the system, are shown in the diagrams from Figure VI-1. up to Figure VI-13. The other obtained results with Skyhook and Ground controllers are shown between Figure VI-14. and Figure VI-25.

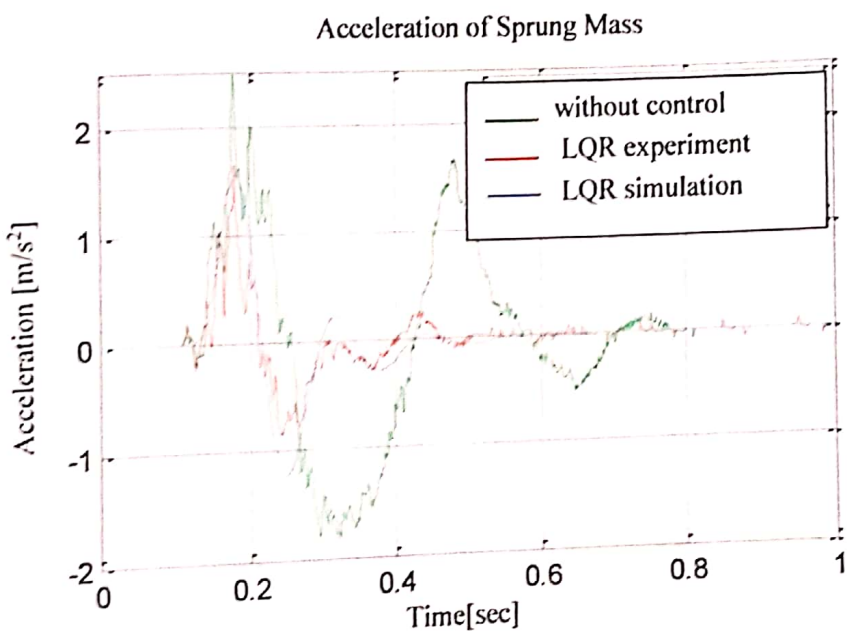


Figure VI-1. Sprung mass acceleration with square wave signal test

According to the first test with LQR controller in the test device, vehicle body acceleration was more successful than passive suspension and simulation.

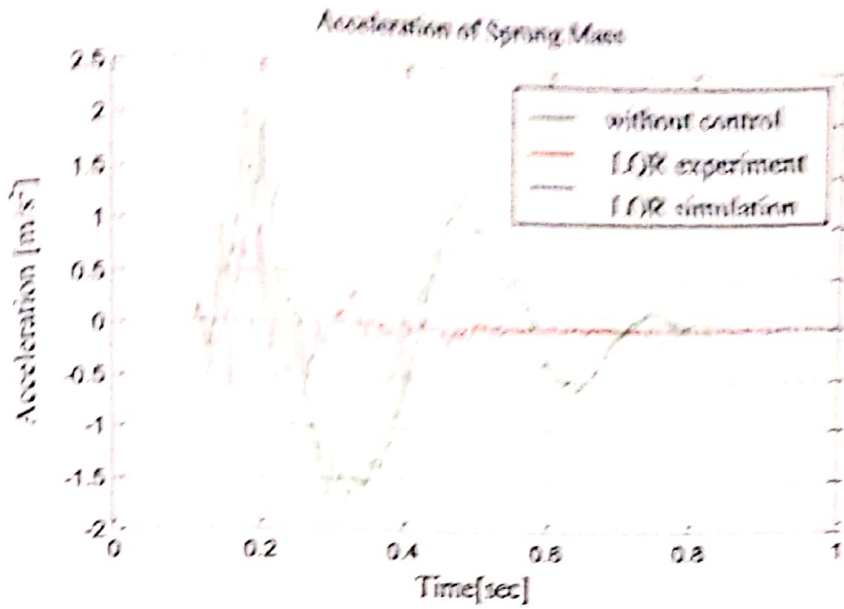


Figure VI-2. Sprung mass acceleration with square wave signal test<sub>2</sub>

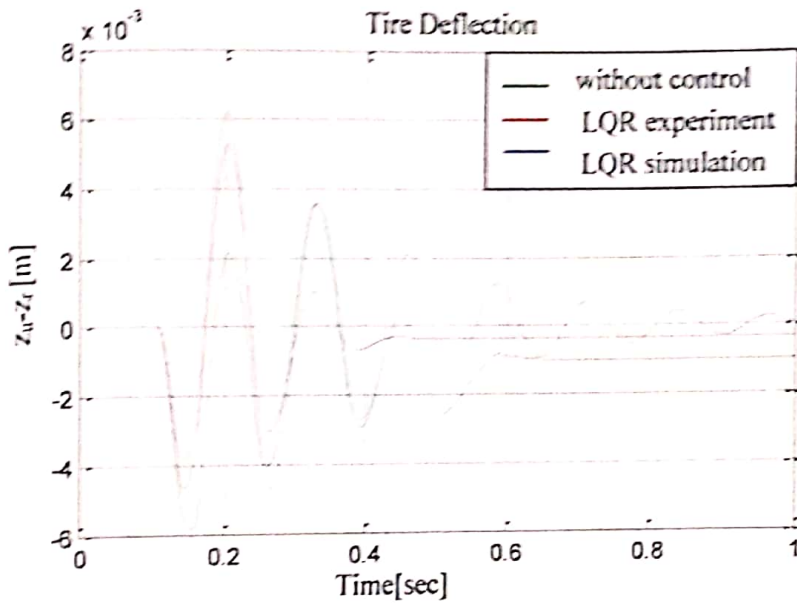


Figure VI-3. Tire Deflection with square wave signal test<sub>2</sub>

According to the second test with LQR controller in the test device, vehicle body acceleration was more successful than passive suspension and simulation. But there is a worse tire deflection than the passive suspension.

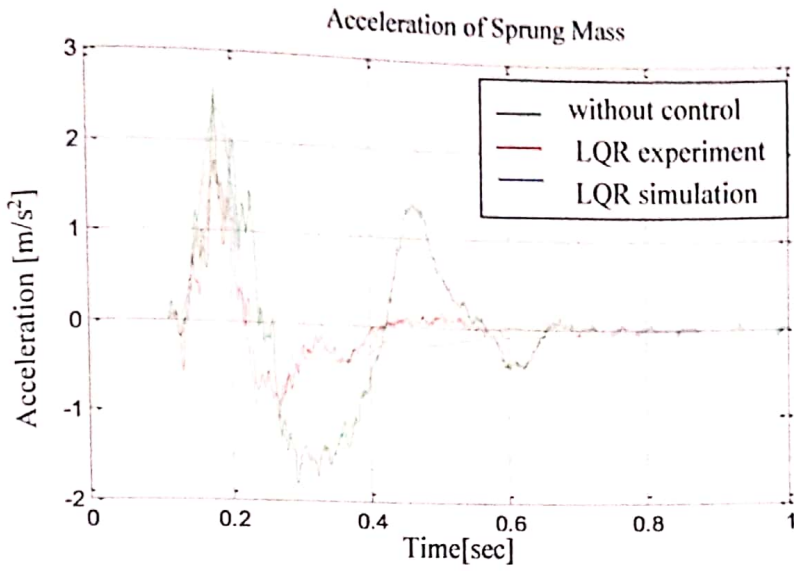


Figure VI-4. Sprung mass acceleration with square wave signal test<sub>3</sub>

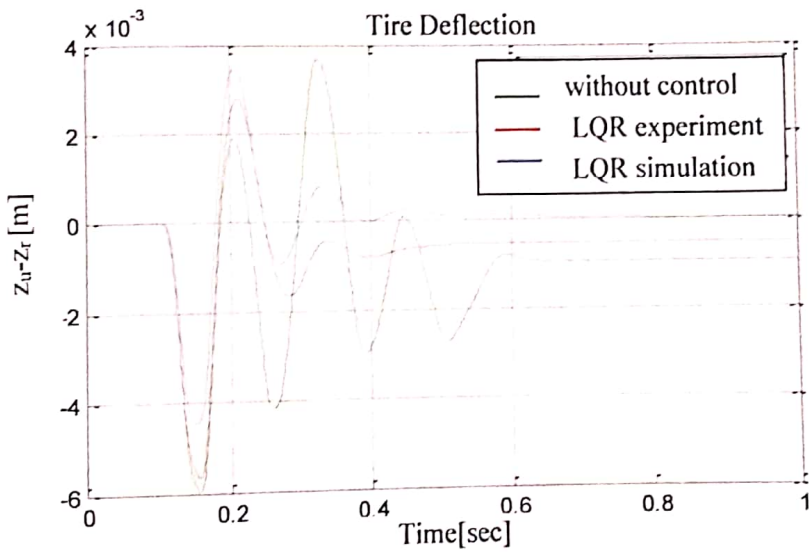


Figure VI-5. Tire Deflection with square wave signal test<sub>3</sub>

When the coefficient of tire deflection is increased, it is seen that successful results are obtained in the amount of tire deflection in the third test result with LQR. However, the same success cannot be seen in the acceleration of vehicle body

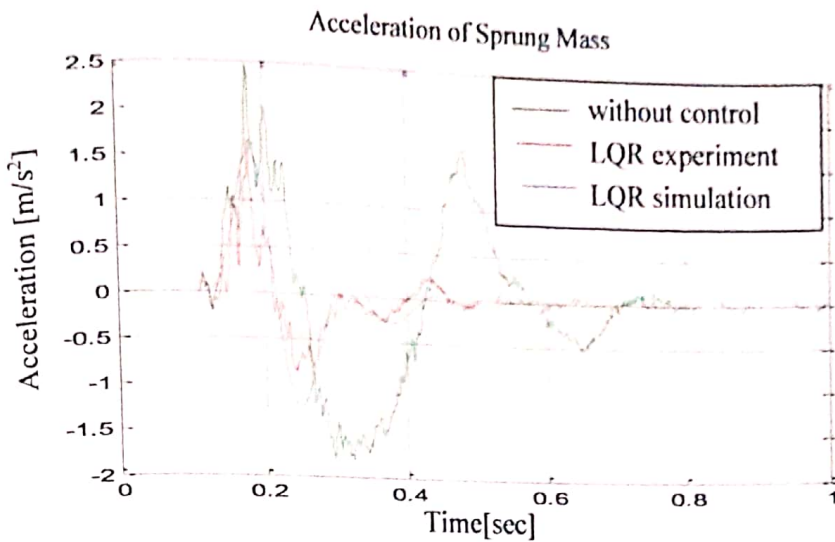


Figure VI-6. Sprung mass acceleration with square wave signal test

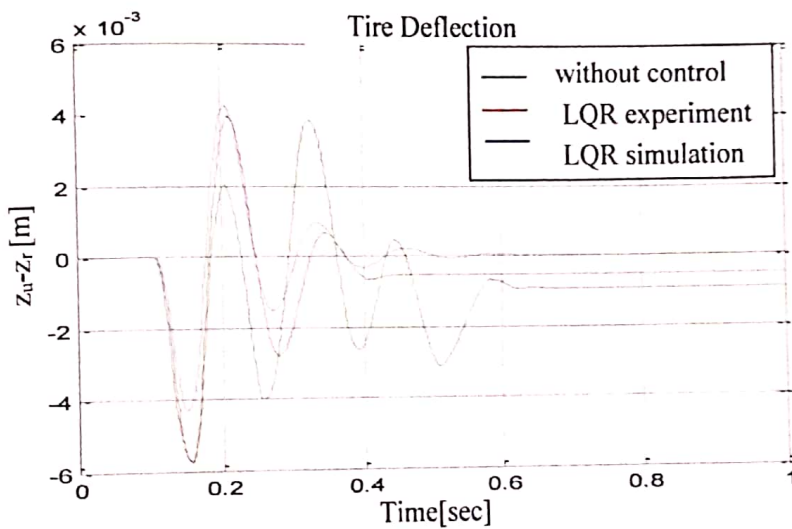


Figure VI-7. Tire Deflection with square wave signal test

The fourth test with LQR shows that when the weighting coefficient of tire deflection and vehicle body acceleration are taken as equal weight, there is a decrease in vehicle body acceleration and tire deflection amount compared to passive suspension.



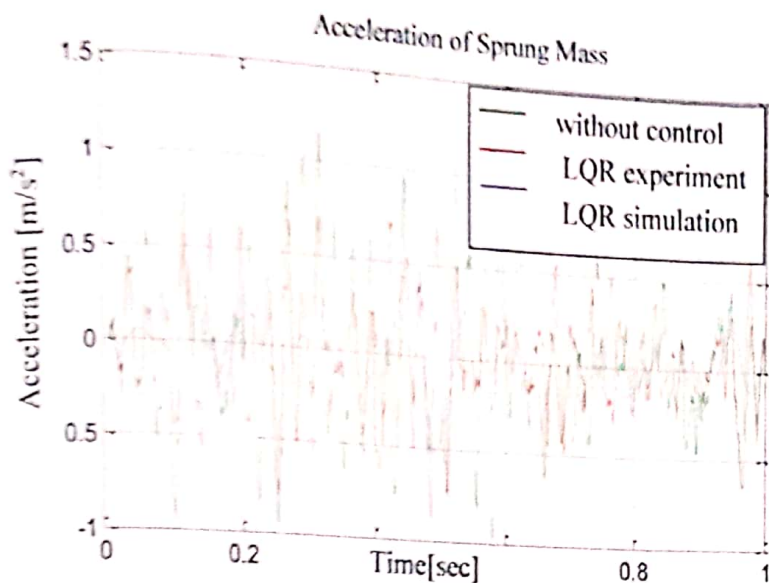


Figure VI-8. Sprung mass acceleration with random signal test<sub>2</sub>

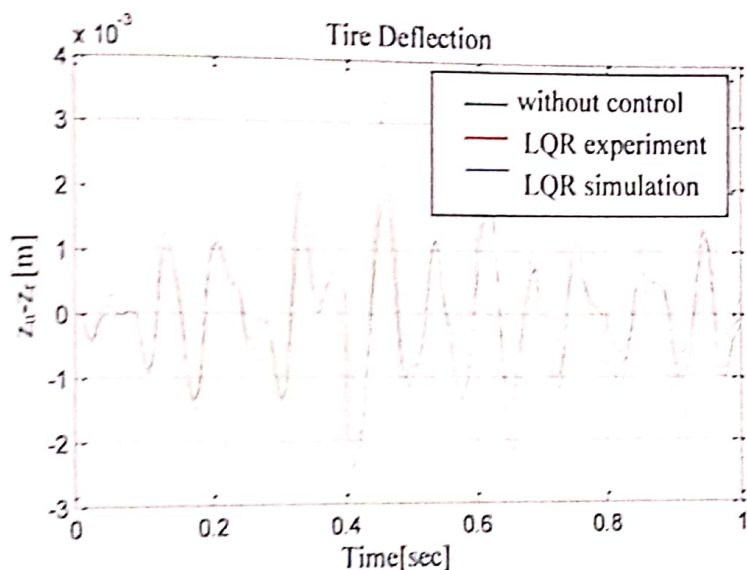


Figure VI-9. Tire Deflection with random signal test<sub>2</sub>

At the random road input of the second test, the acceleration weighted LQR controller is more successful than passive suspension on vehicle body acceleration. However, there is a worse tire deflection with LQR than the passive suspension. The simulation results are more successful in vehicle body acceleration than the experiment. Because there is no damper in the test device.

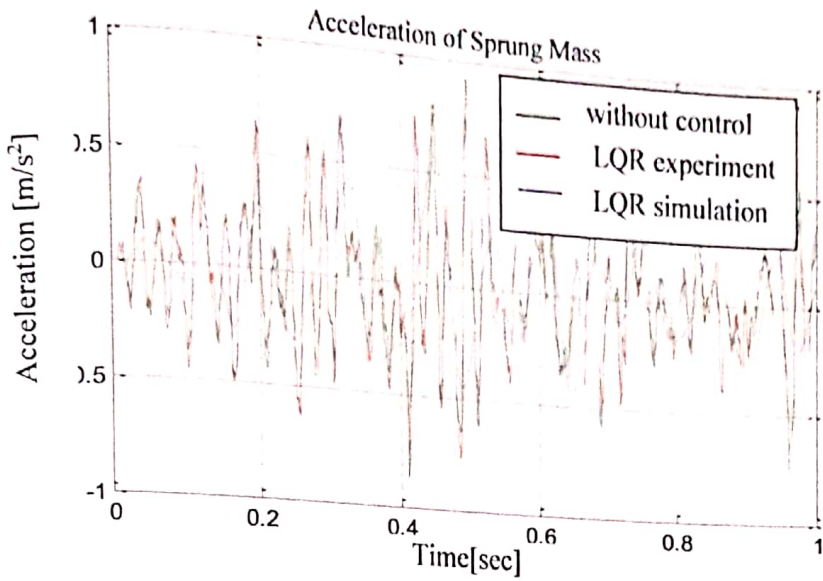


Figure VI-10. Sprung mass acceleration with random signal test<sub>3</sub>

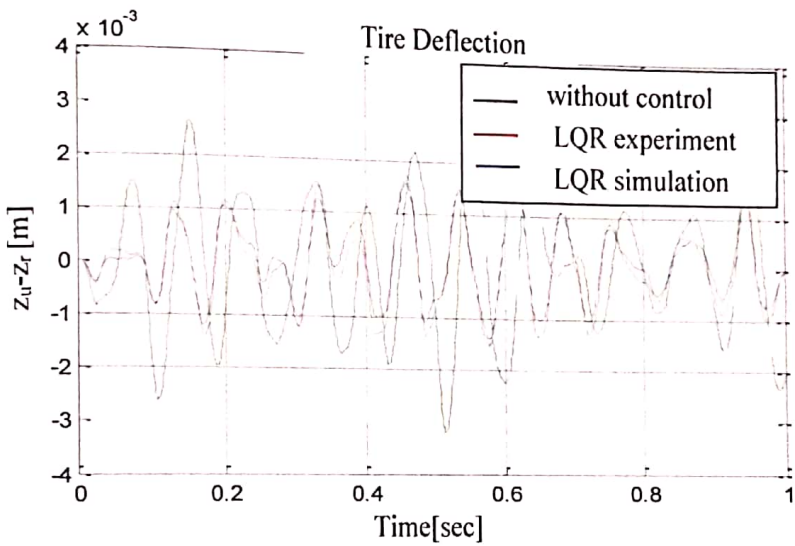


Figure VI-11. Tire Deflection with random signal test<sub>3</sub>

When the coefficient of tire deflection is increased, it is seen that successful results are obtained in the amount of tire deflection in the third test result with LQR. However, the same success cannot be seen in the acceleration of vehicle body. The simulation results are more successful in vehicle body acceleration than the experiment. Because there is no damper in the test device.

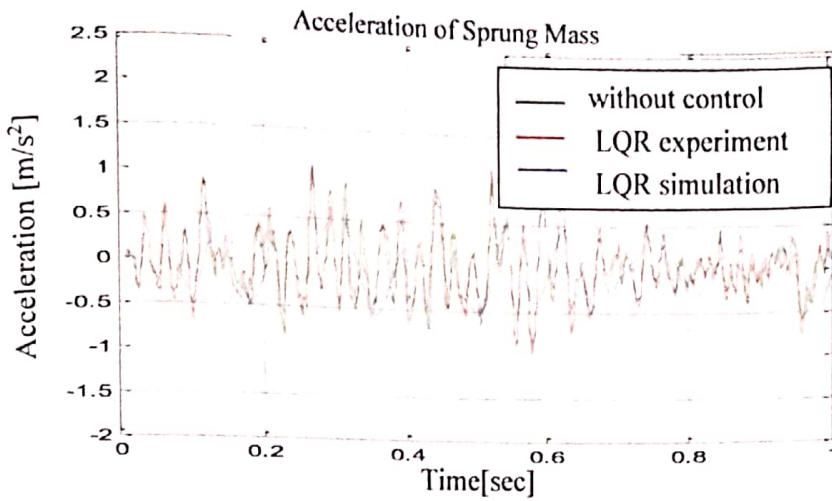


Figure VI-12. Sprung mass acceleration with random signal test4

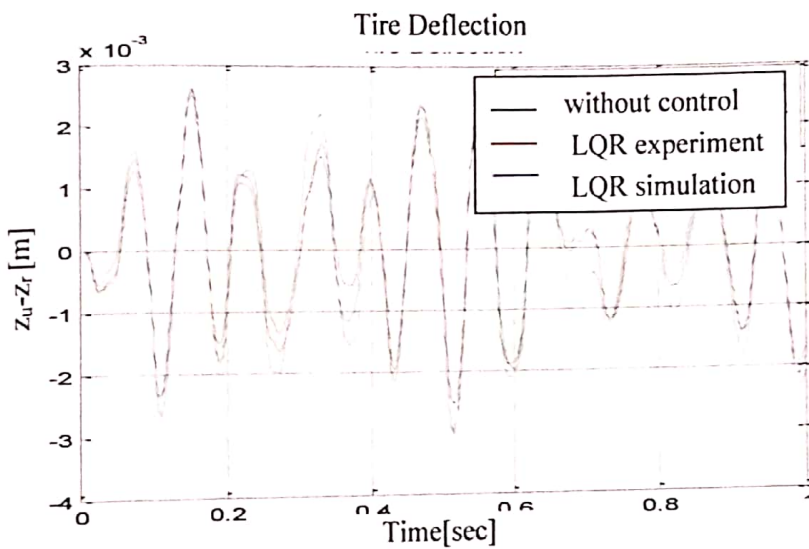


Figure VI-13. Tire Deflection with random signal test4

The results of the equal weighted coefficients of the LQR controller at random road input show that passive suspension is more successful on both vehicle body acceleration and tire deflection than active suspension.

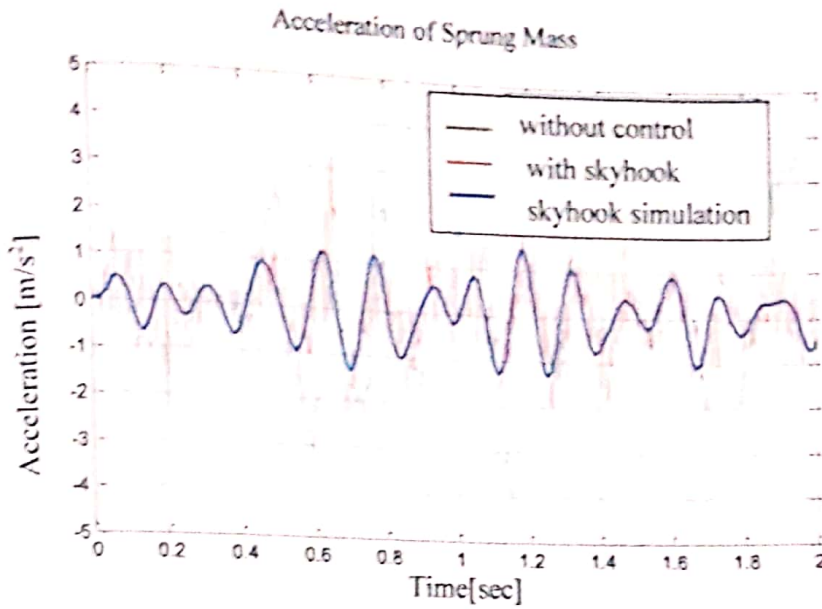


Figure VI-14. Sprung mass acceleration with random signal  $csky=100$

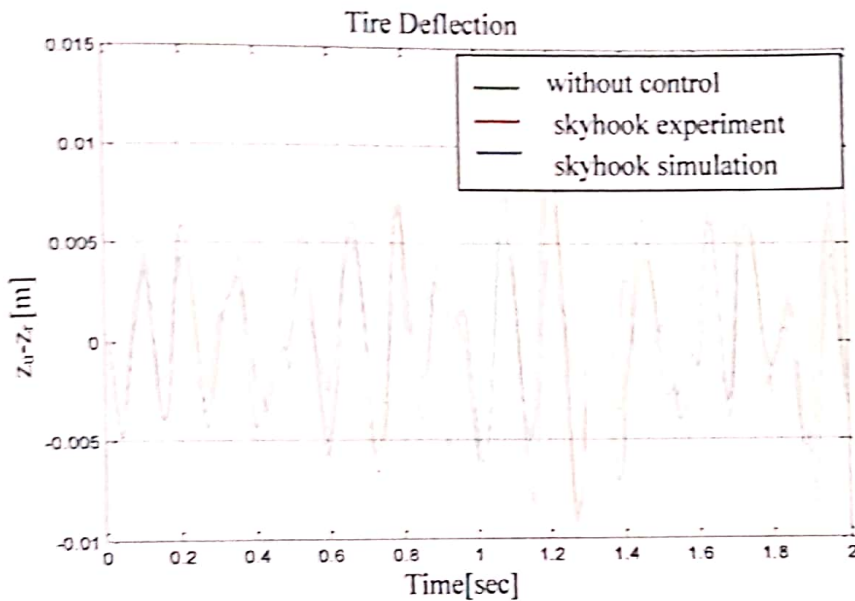


Figure VI-15. Tire Deflection with random signal  $csky=100$

While the skyhook controller at the random input is found to be quite successful on vehicle body acceleration, the same effect cannot be seen in the amount of tire deflection. The simulation results are more successful in vehicle body acceleration than the experiment. Because there is no damper in the test device.

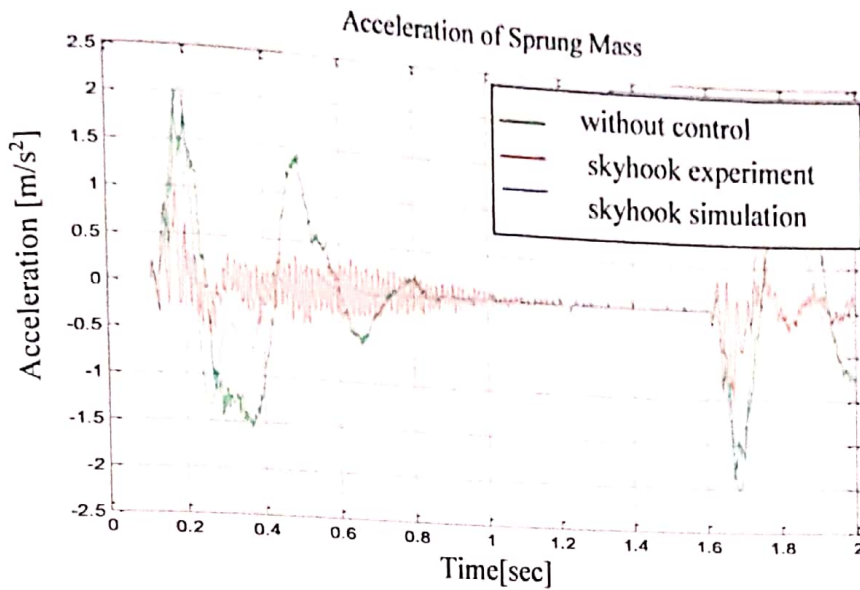


Figure VI-16. Sprung mass acceleration with square wave signal  $csky=100$

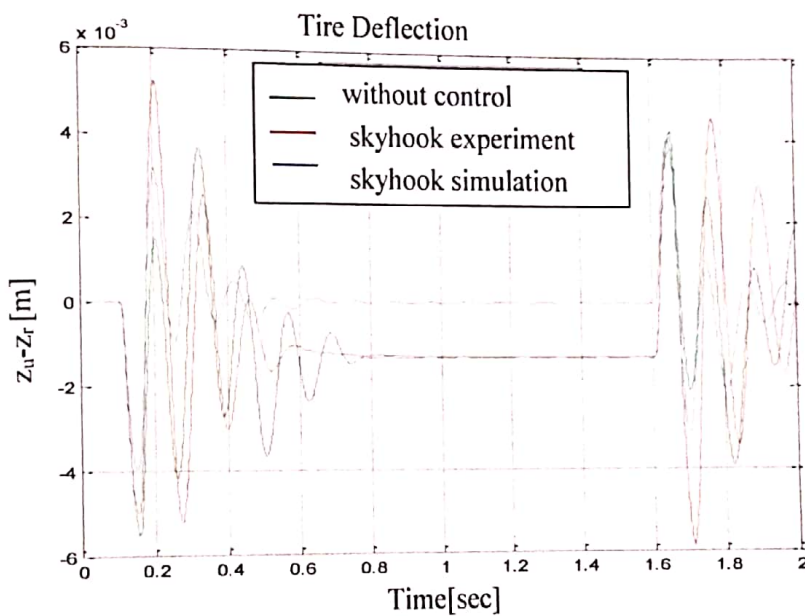


Figure VI-17. Tire Deflection with square wave signal  $csky=100$

According to the second test with skyhook controller at the square wave input in the test device, vehicle body acceleration was more successful than passive suspension and simulation. But there is a worse tire deflection than the passive suspension.

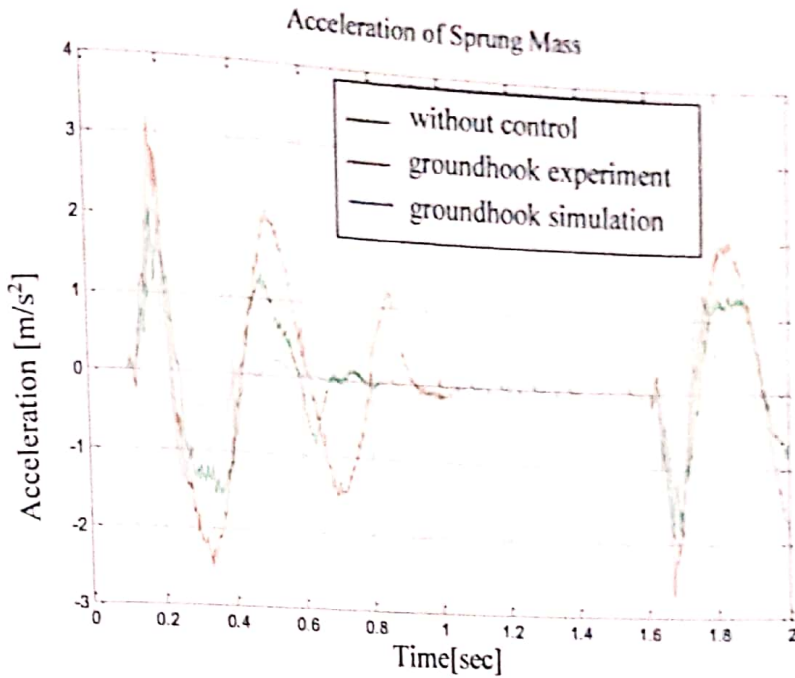


Figure VI-18. Sprung mass acceleration with square wave signal  $cgnd=100$

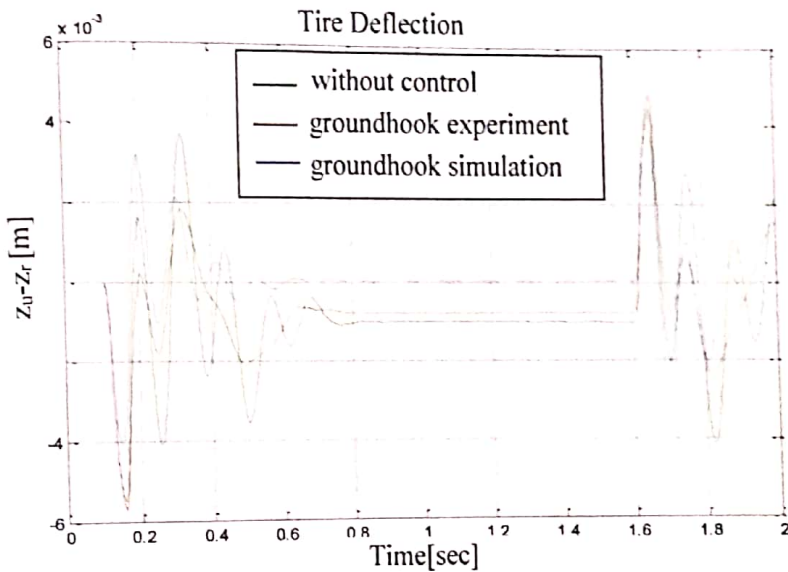


Figure VI-19. Tire Deflection with square wave signal  $cgnd=100$

While the groundhook controller at the square wave input is found to be quite successful in the amount of tire deflection, the same effect cannot be seen on vehicle body acceleration.

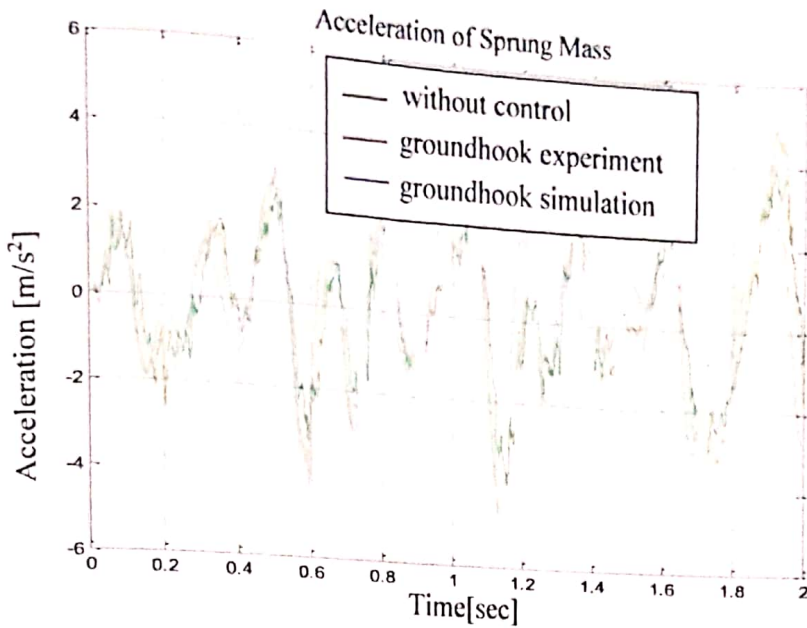


Figure VI-20. Sprung mass acceleration with random signal  $c_{gnd}=100$

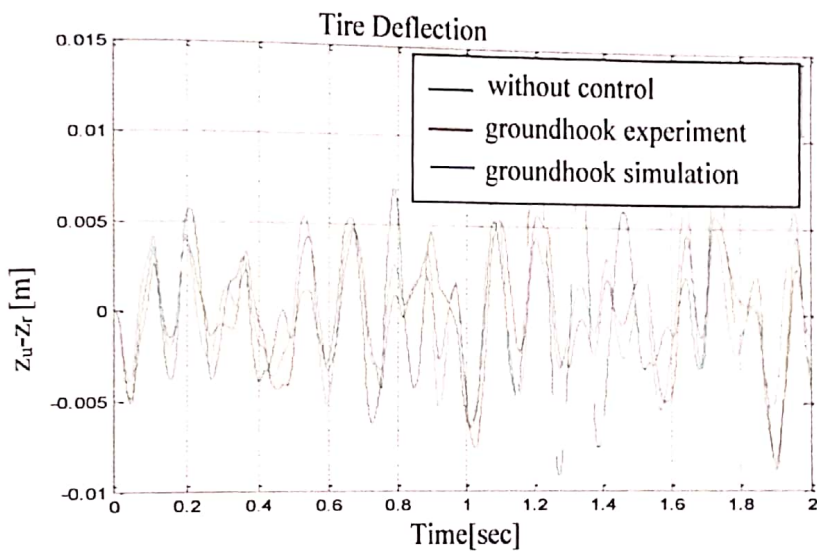


Figure VI-21. Tire Deflection with random signal  $c_{gnd}=100$

According to the second test with groundhook controller at the random road input in the test device, tire deflection amount is successful than passive suspension and simulation. But there is a worse result of vehicle body acceleration than the passive suspension.

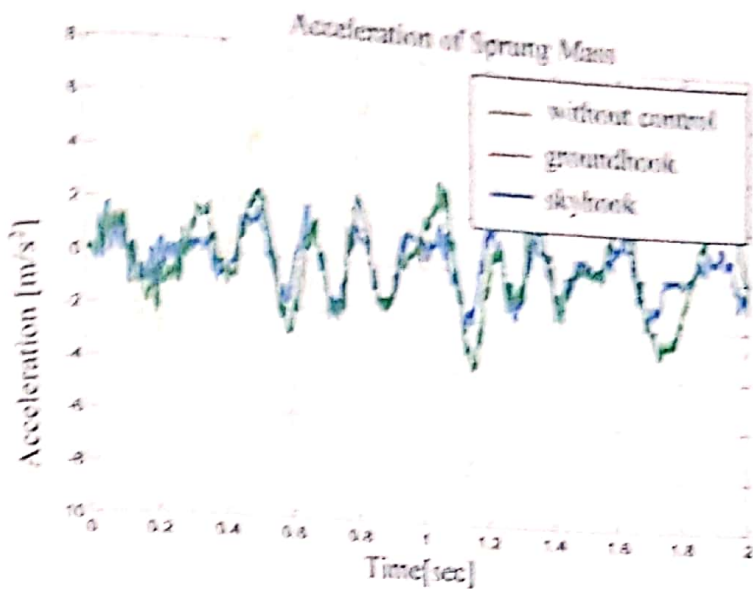


Figure VI-22. Sprung mass acceleration with random signal

$$c_{\text{grd}}=100 \text{ and } c_{\text{sky}}=100$$

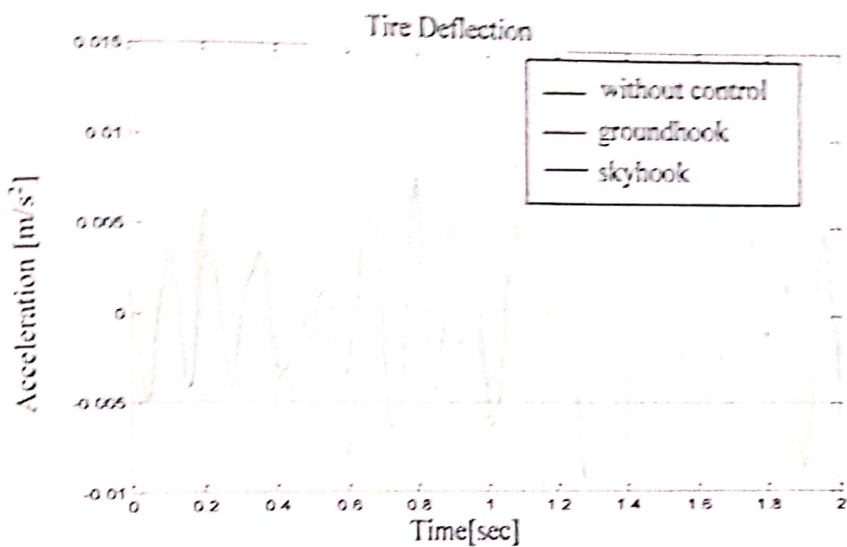


Figure VI-23. Tire Deflection with random signal  $c_{\text{grd}}=100$  and  $c_{\text{sky}}=100$

Comparing the groundhook and skyhook controllers at random road input, the skyhook has a successful effect on vehicle body acceleration while the groundhook controller has a successful effect on the amount of tire deflection.



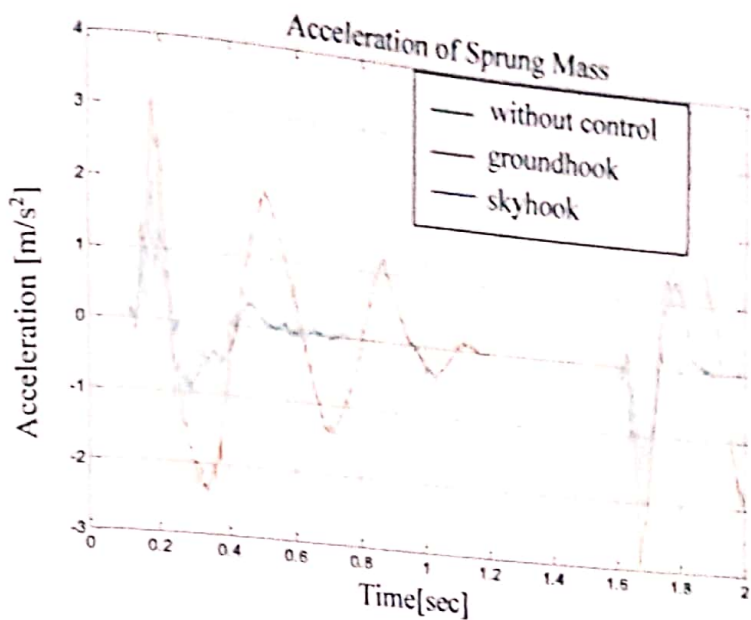


Figure VI-24. Sprung mass acceleration with square wave signal  
 $c_{\text{gnd}}=100$  and  $c_{\text{sky}}=100$

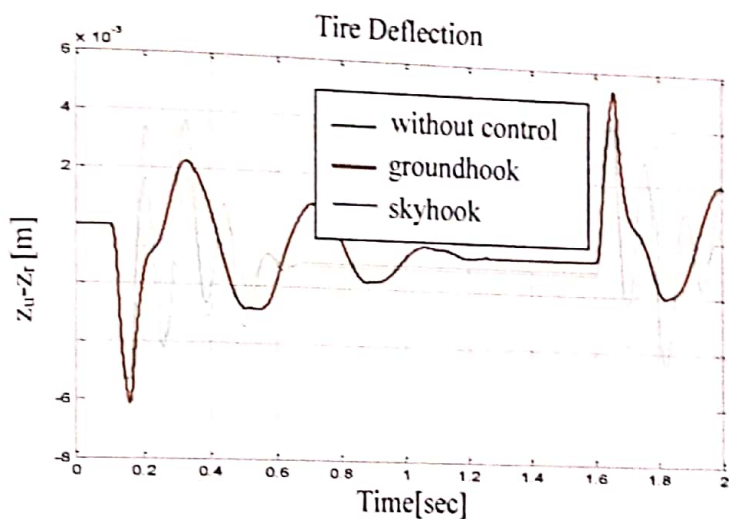


Figure VI-25. Tire Deflection with square wave signal  
 $c_{\text{gnd}}=100$  and  $c_{\text{sky}}=100$

At the random road input, the skyhook has a successful effect on vehicle body acceleration while the groundhook controller has a successful effect on the amount of tire deflection.

## VII. CONCLUSIONS AND RECOMMENDATIONS

Vehicle systems are one of the most affected systems in developing computer and electronic technology. Therefore, many scientists have been working on active suspension systems. In this thesis, active suspension system is examined and controllers are designed to improve driving safety and driving comfort.

In the first part of the thesis, information is given about the suspension systems and horizontal, lateral and vertical movements of the vehicles are mentioned.

In the second part, the Quanser active suspension test device representing the quarter vehicle model used in the proposed study was examined. The parts of the test device are described as what they represent. The numerical values of the parameters of the test device are specified. Matlab simulink program was used as the working environment in the experiments. Quarc toolbox was used to provide the connection between the Quanser active suspension system and MATLAB.

In the third and fourth part of the study, free-body diagrams were shown for quarter vehicle model and mathematical modeling was done by using Newton's laws of motion. The transfer functions of the system and the state-space model were obtained.

In the fifth part of the thesis, information is given about the control of active suspension systems which are the main subject of analysis. Control methods applied in the study are mentioned. Then the model of the active suspension system was removed and the effects of the system parameters were determined. A full state feedback LQR controller was designed using four different parameters of the active suspension system and the performance values of the system were compared to the passive suspension

system. Skyhook and groundhook controllers, which are an alternative method, were designed and simulated according to the parameter change. The performance of the active suspension is evaluated by applying square wave signal and random signal inputs to the system with the designed controllers.

The most important result to be drawn from this study shows that designed controllers have a significant impact on the performance of the active suspension system. This effect is the acceleration of the vehicle body representing driving comfort and the vehicle's road holding is evident on the wheel deflection. It has been observed that the single performance criteria on the active suspension system of the LQR method give more positive results than the multiple performance criteria. The linear control used in this thesis improves one or a maximum two of the performance values, while the third performance value is either improved in certain narrow frequency ranges or completely deteriorated. The Skyhook controller had positive results on vehicle body acceleration, but not on the tire deflection. The Groundhook controller can be well controlled on the tire deflection, while it cannot achieve the same success on acceleration of vehicle body. The effect of combination of Skyhook and Groundhook on active suspension are worse than their individual effects

Improvements can be made by adjusting the performance weighting coefficients. More realistic results could be obtained if the full vehicle model was used instead of the quarter vehicle model used in this study. Considering the overall study, the positive results in the design of the active suspension system will help further studies in the following years.

## REFERENCES

- [1] HeiBing, B. and Ersoy, M., 2011, Chassis Handbook - Fundamentals, Driving Dynamics, Components, Mechatronics, Perspectives. Wiesbaden: Vieweg+Teubner.
- [2] HeiBing, B., 2007, Fahrwerkhandbuch. Wiesbaden: Vieweg Verlag.
- [3] Foda, S. G., 2000, "Fuzzy control of a quarter-car suspension system," Proceedings of the International Conference on Microelectronics, ICM, pp. 231–234.
- [4] Gysen, B. L. J., Paulides, J. J. H., Janssen, J. L. G., and Lomonova, E. A., 2010, "Active electromagnetic suspension system for improved vehicle dynamics," IEEE Transactions on Vehicular Technology, 59(3), pp. 1156–1163.
- [5] Van Der Sande, T. P. J., Gysen, B. L. J., Besselink, I. J. M., Paulides, J. J. H., Lomonova, E. A., and Nijmeijer, H., 2013, "Robust control of an electromagnetic active suspension system: Simulations and measurements," Mechatronics, 23(2), pp. 204–212.
- [6] Fateh, M. M., and Alavi, S. S., 2009, "Impedance control of an active suspension system," Mechatronics, 19(1), pp. 134–140
- [7] Emura, J., S.KakŌzakŌ, F. Yamaoka, M. Nakamura. 1994. Development of the SemiActive suspension System Based on the Sky-Hook Damper Theory, 940863. In: R.K. Jurgen (Editor), Electronic Steering and Suspension Systems (1999), Society of Automotive Engineers, Warrendale-PA, USA, p. 298-306.
- [8] Ahmadian, M. 2001. Active Control of Vehicle Vibration. In: S. Braun, D. Ewins, S.S. Rao (Editors), Encyclopedia of Vibration (2002). Academic Press, San Diego, USA. vol.1, p.37-45

- [9] Agharkakli, A., Sabet, G. S., and Barouz, A., 2012, "Simulation and Analysis of Passive and Active Suspension System Using Quarter Car Model for Different Road Profile," *International Journal of Engineering Trends and Technology*, 3(5), pp. 636–644.
- [10] Reza N. Jazar (2008). *Vehicle Dynamics: Theory and Applications*. Springer, s. 455.
- [11] Huijun Gao and Ping Li, *Handbook of Vehicle Suspension Control System*, 1, The Institution of Engineering and Engineering and Technology, London, United Kingdom, 1, 2014
- [12] Quanser, *Active Suspension User Manual*, 1, Quanser
- [13] <https://whatis.techtarget.com/definition/MATLAB> , accessed at 01.03.2019
- [14] <https://www.quanser.com/products/quarc-real-time-control-software/#overview> , accessed at 04.03.2019
- [15] Yue, C., Butsuen, T., and Hedrick, J. K., 1988. Alternative control laws for automotive suspensions, *Proceedings of the American Control Conference (ACC)*, pp.2373-2378.
- [16] Quanser, *Active Suspension LQG Control using QUARC Instructor Manual*, Quanser
- [17] Rajesh Rajamani, *Vehicle Dynamics and Control*, 1, Springer, Minneapolis, USA, 2, 2012
- [18] Rajamani, R., 2005, *Vehicle Dynamics and Control*, Springer, Minnesota.
- [19] Butsuen, T., 1989. The design of semi active suspensions for automotive vehicles, Ph.D. Dissertation, M.I.T

## APPENDIX

One of the used matlab codes is as follows.

```
% Design of a LQR active damping controller
%parameters

ms=2.45 %Sprung Mass (kg)
mu=1; %Unsprung Mass (kg)
ks=900; %Suspension Stiffness (N/m)
kt=2500; %Tire stiffness
bs=7.5; %Suspension Inherent Damping coefficient
A=[0 1 0 -1;-ks/ms -bs/ms 0 bs/ms;0 0 0 1;ks/mu bs/mu -kt/mu -bs/mu];
B=[0;1/ms;0;-1/mu];
L=[0;0;-1;0];
C=eye(4);
D=zeros(4,1);
Cbody=[0 1 0 0];
Dbody=0;
sysss=ss(A,L,Cbody,Dbody)
bode(sysss);
grid;
hold on
Bfull=[B L];
Dfull=zeros(4,2);
p1=200;
p2=100;
p3=200;
p4=100;
R=1/ms^2;
Q=[(((ks)^2/(ms)^2)+p1) ((bs*ks)/(ms)^2) 0 -
(bs*ks)/(ms)^2;(bs*ks)/(ms)^2 (((bs)^2/(ms)^2)+p2) 0 -(bs)^2/(ms)^2;0
0 p3 0;-(bs*ks)/(ms)^2 -(bs)^2/(ms)^2 0 (((bs)^2/(ms)^2)+p4)];
N=[-((ks)/(ms)^2);-bs/(ms)^2;0;bs/(ms)^2];
[K1] = lqr(A,B,Q,R,N)
sysssc=ss(A-B*K1,L,Cbody, Dbody)
dersys=tf([1 0],1);
sysstf=tf(sysssc)
sysacc=sysstf*dersys
figure
bode(sysssc)
hold
bode(sysacc)
```

The used matlab code for controllability and observability is as follows

```
ms=2.45; %Spring Mass (kg)
mu=1; %Inspring Mass (kg)
ks=900; %Suspension stiffness (N/m)
kt=2500; %Tire stiffness
bs=7.5; %Suspension inherent Damping coefficient
A=[0 1 0 -1; -ks/ms -bs/ms 0 bs/ms; 0 0 1 ks/ms; bs/ms -bs/ms -ks/ms -bs/ms];
B=[0,1/ms;0,-1/mu];
I=[0;0;-1;0];
C=eye(4);
D=zeros(4,1);
Cbody=[0 1 0 0];
Dbody=0;
Co=ctrb(A,B);
unco=length(A)-rank(Co)
Ob=obsv(A,C);
unob=(length(A)-rank(Ob))
```

## VITA

Name Surname : Halil KILIÇ  
Place and Date of Birth : Ankara 03. 04.1980  
Adress : Sinpaş Liva Turkuaz Sitesi Sultanbeyli /İstanbul  
Email : mee.kilie@gmail.com  
High School : Emil Gminder Haus AGR Reutlingen/Germany  
B.Sc : Reutlingen University and Okan University  
Mechatronics  
M.Sc. : Gedik University Occupational Health and Safety